UNIVERSITY OF CALIFORNIA SANTA CRUZ

CHARACTERIZING INHIBITORS OF THE BACTERIAL TYPE THREE SECRETION SYSTEM

A dissertation submitted in partial satisfaction of the requirements for the degree of

DOCTOR OF PHILOSOPHY

in

CHEMISTRY
with an emphasis in MICROBIOLOGY and ENVIRONMENTAL TOXICOLOGY

by
Jessica M. Morgan
September 2018

The Dissertation of Jessica M. Morgan is approved:

Professor Victoria Auerbuch Stone

Professor Scott Lokey, chair

Professor John MacMillan

Lori Kletzer
Vice Provost and Dean of Graduate Studies

TABLE OF CONTENTS

TABLE OF CONTENTS iii

ABSTRACT vi

DEDICATION AND ACKNOWLEDGEMENTS vii

CHAPTER 1 1

Assays to probe T3SS assembly and activity 1

INTRODUCTION 2

GENE EXPRESSION 4

STRUCTURAL ASSEMBLY 5

SECRETION 6

HOST CELL DAMAGE 7

TRANSLOCATION 8

DISCUSSION 10

REFERENCES 12

CHAPTER 2 19

An experimental pipeline for initial characterization of bacterial type III secretion system inhibitor mode of action using enteropathogenic *Yersinia* .....

By: Jessica Morgan, Jocelyn Delgado, Hanh Lam, Justin Luu, Sina Mohammadi, Ralph R. Isberg, Helen Wang, and Victoria Auerbuch .....

ABSTRACT: **20**

INTRODUCTION **21**

MATERIALS AND METHODS **24**

RESULTS **34**

T3SS inhibitor training set for assay pipeline 35

Assessment of T3SS gene expression 40

Assessment of T3SS assembly 45

Assessment of effector protein translocation 49

DISCUSSION **50**

ACKNOWLEDGEMENTS **54**

REFERENCES **55**

CHAPTER 3 ..... **63**

Piericidin A1 Blocks Yersinia Ysc Type III Secretion System Needle Assembly ....

By: Jessica M. Morgan, Miles C. Duncan, Kevin S. Johnson, Andreas Diepold, Hanh Lam, Allison J. Dupzyk, Lexi R. Martin, Weh Ruh Wong, Judith P. Armitage, Roger G. Linington, Victoria Auerbuch .....

ABSTRACT **64**

INTRODUCTION **65**

MATERIALS AND METHODS **67**

RESULTS **75**

Complex I inhibition by piericidin does not underlie its ability to block type III secretion 75

Piericidin A1 inhibits the *Y. pseudotuberculosis* and *Y. enterocolitica* Ysc T3SS, but not

the *Y. enterocolitica* Ysa T3SS 79

Piericidin A1 traps T3SS effector proteins inside bacterial cells independently of the YopN, YopD, and YopK T3SS regulatory proteins 81

Piericidin A1 decreases the number of T3SS needles associated with the bacterial surface but does not alter localization of basal body components 85

Piericidin A1 blocks YscF higher order structure formation and decreases secretion of middle and late T3SS substrates 88

Piericidin A1 inhibition of type III secretion is reversible, and this reversibility is independent of new protein synthesis 89

DISCUSSION 91

ACKNOWLEDGEMENTS 95

REFERENCES 96

ABSTRACT

Jessica M. Morgan

Characterizing Inhibitors of the Bacterial Type Three Secretion System

The aims of my dissertation research were to characterize the activity of inhibitors targeting the bacterial virulence factor, the type III secretion system (T3SS). The T3SS is a needle-like apparatus used by dozens of bacterial pathogens to directly deposit bacterial effector toxins inside the cytoplasm of target host cells. This virulence factor is typically essential for bacterial survival and replication within the host, and dozens of T3SS- positive pathogens are the causative agents of relevant health threats. Importantly, these T3SSs are highly conserved between bacterial species that possess them, making them an attractive potential drug target. The first half of this work focuses on taking advantage of the tightly regulated, processional assembly and deployment of the T3SS and designing and optimizing assays we can use to probe for inhibitory activity at discreet stages throughout this process.

The second goal of my dissertation research was to employ this assay to characterize an inhibitor of the T3SS, piericidin A1, and have determined the molecule inhibits T3SS needle assembly.

DEDICATION AND ACKNOWLEDGEMENTS

To my incredible husband and son – None of this would have been possible without your love, support and patience- thank you. I love you both more than you will ever know. Benji, my SONshine. I want you to know that you can achieve anything if you're willing to persevere and work hard.

To my parents, brother, and sisters who have supported me, cheered me on, made the long drives, and have- without wavering- loved me these past five years (well, forever, really) – thank you. I am so honored that I belong to our clan.

To my inlaws, nieces and nephews- Thank you all for believing in me, supporting Andy and I and making the long trips to see us! We love you.

To all of my amazing friends- I can't put into works how grateful I am to you all for the laughs, the shoulders to cry on and the constant encouragement, yI cherish each and every one of you.

To my 'sisters' Linnea, Caileen and Jolene – Our friendship is something I will treasure as long as I live, and I'm so grateful this experience brought us together. Thank you for always being by my side.

To Vicki Auerbuch Stone – thank you for being an OUTSTANDING example of a woman in science, an unbelievably supportive and inspiring mentor, for pushing me and molding me into the scientist I will leave having become. I will forever aspire to balance family and science with the grace you do.

To my undergrads (Lexi and Jocelyn) – thank you for all your hard work and dedication. I'm so grateful I was able to be your mentor.

To all the grads and postdocs of the lab, past and present (Walter, Miles, Leah, Hanh, Diana, David, Yahan and Kate) – You're all a STONE cold pack of weirdos and I'm so grateful for each and every one of you.

To all the lab undergrads (Natalia, Allie, Kevin, and Olivia, Justin and Cameron) – Thank you for being hard working, fun and keeping our environment friendly.

To my thesis committee – thank you for your guidance throughout this process

Chapters 2 and 3 of this dissertation are multi-author publications. I am responsible for all figures except: Figures 1B and S3 in chapter 3.

CHAPTER 1

Assays to probe T3SS assembly and activity

By Jessica M Morgan and Victoria Auerbuch

INTRODUCTION

Pathogenic *Yersinia* species, in addition to dozens of other Gram negative pathogens, utilize a type three secretion system (T3SS) to translocate bacterial effector proteins into host cells and modulate host defenses. The T3SS resembles a molecular syringe and is specialized for protein export, allowing for deposition of toxins directly into target cells (Cornelis 2010). The T3SS is well conserved among more than twenty-five species of Gram-negative bacteria, most of which are pathogenic to plants and mammals. Assembly of this machine occurs in a tightly regulated, hierarchical fashion. A number of T3SS-encoding bacteria are facultative pathogens, and only express the T3SS during the host-associated part of their life cycle. Because of the high energetic cost of building and utilizing the T3SS, these bacteria tightly regulate T3SS expression in response to environmental cues. For example, pathogenic *Yersinia* encode the Ysc T3SS on the pYV virulence plasmid and pYV copy number increases in host animals (Wang et al. 2016). The pYV virulence plasmid encodes the T3SS master regulator, LcrF, which drives expression of T3SS genes. Expression of LcrF is controlled by temperature, several other transcription factors that respond to cell stress as well as iron and oxygen levels, and T3SS activity (Schwiesow et al. 2015).

The initial stage of T3SS deployment involves assembly of the basal body structure in the bacterial cell envelope, beginning with integration of the secretin YscC in the outer membrane (OM) and oligomerization of the inner membrane rings,

YscD and YscJ (Diepold et al. 2010). Upon completion of the basal body, helical polymerization of a monomeric needle subunit, YscF, forms the T3SS needle. The YscF needle forms a hollow conduit through which T3SS effector proteins are secreted in an unfolded manner, en route to the host cell (Radics et al. 2014). Post needle polymerization, the needle is capped by LcrV and oligomerizes with two pore forming proteins, YopB and YopD, to form a translocon pore complex in the host plasma membrane (Costa et al. 2010; Mattei et al. 2011). After contact has been made with the host plasma membrane, a substrate specificity switch occurs and transitions to secretion of late effectors. These T3SS substrates are targeted to the secretion machinery through an N-terminally contained secretion signal (Lloyd et al. 2001). The underlying mechanism on specificity of T3SS targeting via the N- terminal signal is not completely known, but data supports that it lies in a combination of amino acid content, secondary structure and solvent accessibility (Wang et al. 2013). Additionally, many T3SS substrates are accompanied (maybe I should say guided?) to the export machinery by chaperones which prevent premature folding in the bacterial cytoplasm (Trülzsch et al. 2003). Once in the host cytoplasm, the effectors modulate host pathways to subvert host defense mechanisms. While the T3SS itself is well-conserved, the repertoire of T3SS effectors differs significantly between species (Troisfontaines and Cornelis 2005). In the case of *Yersinia,* extracellular pathogens, the effector proteins inhibit phagocytosis and recognition by the host immune system (Pha and Navarro 2016).

Since the discovery of the apparatus and our understanding of its importance

to cause successful infections, researchers have needed to develop ways to study its activity, both *in vivo* and *in vitro*. The ability to study T3SS activity throughout its deployment process has provided unprecedented insights into its regulation and assembly; however, many techniques have their drawbacks and limitations. Our ability to sensitively and accurately interrogate T3SS gene expression, structural assembly, secretion, host cell contact, and translocation is essential in driving discovery forward. This review provides a summary of the assays that have been developed to probe this complex nanomachine.

GENE EXPRESSION

A variety of techniques are available to researchers for studying expression of T3SS genes. Perhaps the most commonly used and accepted methods to assess T3SS gene expression are qRT-PCR and whole transcriptome analysis using RNA-seq or microarrays. Microarray analysis has been applied in attempting to elucidate the mechanism of action a member of the salicyladine acylhydrazides class of T3SS inhibitors in *E.* coli, and revealed that they seem to be broadly effecting virulence genes, and are potentially targeting a global virulence regulator (Tree et al. 2009). The benefit of these techniques is ability to use any bacterial strain (no need to construct reporter strains, for example). The main drawback of this technique is that it is very low throughput and time intensive.

In order to analyze the expression of only a specific subset of T3SS-associated genes, a variety of genetic approaches, typically capitalizing on fluorescent or

luminescent reporters, can be used. Using transcriptional reporters to probe T3SS gene expression have the advantage of being amenable to miniaturization and high throughput screening. In fact, the first published screen for T3SS inhibitors utilized a transcriptional reporter for the *Yersinia pseudotuberculosis* gene yopE (Kauppi et al. 2003). Drawbacks of this technique includes sensitivity and saturation. For example, we found that only T3SS inhibitors that inhibit secretion of effectors >90% significantly inhibit *yopE* expression (see Chapter 2).

STRUCTURAL ASSEMBLY

Visualizing structural components of the T3SS has been a challenge in the field, as the T3SS is a >300 megadalton apparatus that spans two bacterial membranes and makes contact with the eukaryotic target cell membrane. Some of the earliest structural studies of the apparatus come from visualization of purified T3SS structures from *Salmonella* by electron microscopy (Kubori et al. 1998). While these purified particles offered important initial insight into the supramolecular structure of the T3SS, more recent work demonstrated that the T3SS export apparatus is lost when isolating T3SS from bacteria (Hu et al. 2017; Hu et al. 2015). More recently, cryo-electron tomography has been applied, allowing researchers to observe the T3SS *in situ* (Hu et al. 2017; Nans et al. 2015). In addition, cryo-electron microscopy has been used to observe T3SSs with an effector substrate trapped in the needle, demonstrating its transit through the T3SS in a partially unfolded, directional manner (Dohlich et al. 2014; Radics et al. 2014).

A common genetic approach that has been applied to explore localization, and order of incorporation for T3SS structural proteins has been through tagging functional structural components with fluorescent molecules, like GFP or mCherry. Studies utilizing fluorescent proteins have been integral in helping the field appreciate the dynamic nature of the T3SS structural components (Diepold et al. 2015; Diepold et al. 2011). Another commonly used technique for visualizing some of the extracellular components, like LcrV and YscF, has been the use of immunofluorescence. By raising an antibody to the antigen of interest, localization of proteins can be determined using fluorescence microscopy (Davis et al. 2010; Morgan et al. 2017).

SECRETION

A simple yet powerful assay to assess T3SS-dependent protein secretion is by inducing type III secretion in the absence of host cells and precipitating secreted proteins with trichloroacetic acid. The conditions for inducing type III secretion in the absence of host cells have been elucidated for only a subset of T3SS-expressing bacteria. For reasons that remain clear, removal of calcium from bacteriological media triggers type III secretion in *Yersinia* (Mehigh et al. 1989; Straley and Bowmer 1986). After triggering secretion *in vitro* (low calcium, 37˚C) secreted *Yersinia* effector proteins (Yops) precipitated from the supernatant can be separated on a polyacrylamide gel and stained with Coomassie blue or visualized by immunoblotting. The main drawback for analyzing the secretome in this fashion is

that it requires several mL of culture, not ideal in applications where miniaturization is desired or small volumes required.

A variation on this secretion assay that requires a much smaller volume involves a chimeric T3SS effector reporter fused to the TEM1 ß-lactamase domain lacking its secretion signal. Secretion can be triggered *in vitro* and secreted ß-lactamase activity can be measured by hydrolysis of a chromogenic ß-lactamase substrate such as nitrocefin. This technique has been very useful in bulk screening efforts looking for inhibitors of T3SS secretion (Aiello et al. 2010).

A more focused approach that has been demonstrated in *Pseudomonas* exploits the native enzymatic activity of individual effector proteins (Rolsma and Frank 2014). One example is ExoU, a secreted A_2 phospholipase from *Pseudomonas* that targets cell membranes. Secretion of ExoU can be measured *in vitro* through its ability to cleave an extracellular florigenic substrate, PED6 (Benson et al. 2010).

HOST CELL DAMAGE

T3SS-mediated pore formation in the eukaryotic membrane can result in leakage of host cell intracellular components (Dacheux et al. 2001). In addition, some translocated effectors are toxic to eukaryotic cells and their translocation results in cell lysis (Chatterjee et al. 2015; Faudry et al. 2013). It is therefore possible to monitor T3SS-dependent membrane disruption and/or effector-mediated host cell killing by assessing the presence of cytoplasmic components in infection supernatants. Some studies have monitored the release of endogenous host enzymes

or exogenously added dyes. Lactate dehydrogenase (LDH) is an endogenous enzyme found in the cytoplasm of healthy eukaryotic cells. Upon membrane disruption cell death, LDH is released into the supernatant. Increased LDH activity in culture supernatant is proportional to cell membrane damage, and can be quantified through a coupled enzymatic reaction converting a tetrazolium salt, INT, to a red formazan product measured spectroscopically. In a similar technique, a cell permeable dye BCECF-AM [2′,7′-bis-(2-carboxyethyl)-5 (and 6)-carboxyfluorescein] can be loaded into a monolayer of cells. Once in the eukaryotic cytoplasm, it is cleaved by endogenous esterases, becoming fluorescent and cell impermeable. Only upon membrane disruption and/or osmotic lysis is the dye able to be released into the culture supernatant, and measured spectroscopically (Marenne et al. 2003).

Another popular technique that has been applied to measure T3SS-dependent host membrane disruption is the red blood cell (RBC) lysis assay. RBC membrane rupture leads to hemoglobin release, which can be monitored spectroscopically. The amount of hemoglobin in the supernatant correlates with T3SS dependent cell contact (Sansonetti et al. 1986).

TRANSLOCATION

One of the earliest techniques to measure effector translocation was designed around the cytotoxic ‘cell rounding’ response seen in cells infected with a T3SS pathogen expressing an actin cytoskeleton disrupting T3SS effector protein (Miura et al. 2006; Rosqvist et al. 1990). In the case of *Yersinia,* infection of a cell monolayer

results in host cells losing their distinct cell shape and rounding up due to activity of YopE, a Rho GTPase activating protein (GAP), which modulates Rac-dependent actin structures in eukaryotic cells (Andor et al. 2001). In earlier studies, quantitation of cell monolayer rounding was done by eye in a semi-quantitative manner (Felek et al. 2010; Krall et al. 2004). More recently, image analysis software has been used to provide a more quantitative measurement of cell rounding using metrics such as cell area (Harmon et al. 2010).

Cell fractionation and Western blotting can also be employed to evaluate translocation of T3SS effectors into host cells. After infection and washing of a cell monolayer, cells can be lifted, lysed, and probed for the presence host cell-associated T3SS effectors. An improvement on the specificity of this technique requires the fusion of a glycogen synthase kinase (GSK) tag to a translocated effector protein (Garcia et al. 2006). When this chimeric protein is translocated into the host cell, the GSK tag is phosphorylated by endogenous protein kinases, and the phosphorylated tag can be detected with a GSK-3ß antibody. This technique conforms that the effector has been deposited into the host cytoplasm.

The most common method for monitoring translocation of T3SS and T4SS effector proteins is a FRET based ß-lactamase approach. A chimeric effector-reporter can be generated by fusion of a T3SS effector protein to the TEM1 ß-lactamase domain lacking its secretion signal. After infection, the eukaryotic cell monolayer is treated with CCF2-AM a cell permeant ß-lactamase substrate that enters into the cell freely, but is cleaved after entry by cytoplasmic esterases and cannot diffuse out. The

dye undergoes FRET and fluoresces green when uncleaved. If the chimeric effector was successfully translocated, CCF2 will be cleaved, FRET will be lost, and the dye will emit blue fluorescence (Charpentier and Oswald 2004). The main drawback of this approach is the cost of the CCF2-AM reagent, limiting use of this technique to smaller scale experiments.

An alternative approach is an adenylate cyclase (Cya) reporter assay (Chakravarthy et al. 2017). This assay also requires the generation of a chimeric reporter-effector, fusing an effector with the calmodulin-dependent adenylate cyclase domain of CyaA. Once the effector is translocated into the target cell, it is activated by its cofactor, calmodulin, and can catalyze the conversion of adenosine triphosphate (ATP) to cyclic adenosine monophosphate (cAMP). cAMP levels can then be measured with an enzyme-linked immunosorbent assay (ELISA) kit using a cAMP specific antibody.

DISCUSSION

Development of techniques to analyze T3SS activity and function is still an actively growing space. As our understanding of the T3SS grows, our need for improved techniques with improved sensitivity must grow in kind. While most techniques come with some drawbacks and limitations, the repertoire of tools we have at our disposal in the field today allows a researcher to answer just about any scientific question.

In general, straightforward techniques to assess different stages of type III

secretion that can be miniaturized and made amenable to screening are highly useful and desired in our field. These types of techniques support forward genetic screening approaches on mutagenized libraries to assess specific phenotypes, or allow for screening of molecules that might inhibit a particular process during T3SS assembly or secretion. Therefore, further development of such techniques should be a focus going forward.

One example of how miniaturized assays would benefit the field lies in defining activity of virulence blockers. Inhibiting the activity of the T3SS has become a promising avenue for next generation antimicrobials (Duncan et al. 2012), and while many novel inhibitors have been discovered, very few have been characterized. Using a combination of the techniques described here provides an opportunity for characterizing behavior of these inhibitors in a broader context than has been explored before.

REFERENCES

Aiello D, Williams JD, Majgier-Baranowska H, Patel I, Peet NP, Huang J, Lory S, Bowlin TL, Moir DT. 2010. Discovery and characterization of inhibitors of pseudomonas aeruginosa type iii secretion. Antimicrob Agents Chemother. 54(5):1988-1999.

Andor A, Trülzsch K, Essler M, Roggenkamp A, Wiedemann A, Heesemann J, Aepfelbacher M. 2001. Yope of yersinia, a gap for rho gtpases, selectively modulates rac-dependent actin structures in endothelial cells. Cell Microbiol. 3(5):301-310.

Benson MA, Schmalzer KM, Frank DW. 2010. A sensitive fluorescence-based assay for the detection of exou-mediated pla(2) activity. Clin Chim Acta. 411(3-4):190-197.

Chakravarthy S, Huot B, Kvitko BH. 2017. Effector translocation: Cya reporter assay. Methods Mol Biol. 1615:473-487.

Charpentier X, Oswald E. 2004. Identification of the secretion and translocation domain of the enteropathogenic and enterohemorrhagic escherichia coli effector cif, using tem-1 beta-lactamase as a new fluorescence-based reporter. J Bacteriol. 186(16):5486-5495.

Chatterjee A, Caballero-Franco C, Bakker D, Totten S, Jardim A. 2015. Pore-forming activity of the escherichia coli type iii secretion system protein espd. J Biol Chem. 290(42):25579-25594.

Cornelis GR. 2010. The type iii secretion injectisome, a complex nanomachine for intracellular 'toxin' delivery. Biol Chem. 391(7):745-751.

Costa TR, Edqvist PJ, Bröms JE, Ahlund MK, Forsberg A, Francis MS. 2010. Yopd self-assembly and binding to lcrv facilitate type iii secretion activity by yersinia pseudotuberculosis. J Biol Chem. 285(33):25269-25284.

Dacheux D, Goure J, Chabert J, Usson Y, Attree I. 2001. Pore-forming activity of type iii system-secreted proteins leads to oncosis of pseudomonas aeruginosa-infected macrophages. Mol Microbiol. 40(1):76-85.

Davis AJ, Díaz DA, Mecsas J. 2010. A dominant-negative needle mutant blocks type iii secretion of early but not late substrates in yersinia. Mol Microbiol. 76(1):236-259.

Diepold A, Amstutz M, Abel S, Sorg I, Jenal U, Cornelis GR. 2010. Deciphering the assembly of the yersinia type iii secretion injectisome. The EMBO journal. 29(11):1928-1940.

Diepold A, Kudryashev M, Delalez NJ, Berry RM, Armitage JP. 2015. Composition, formation, and regulation of the cytosolic c-ring, a dynamic component of the type iii secretion injectisome. PLoS biology. 13(1):e1002039.

Diepold A, Wiesand U, Cornelis G. 2011. The assembly of the export apparatus (yscr,s,t,u,v) of the yersinia type iii secretion apparatus occurs independently of other structural components and involves the formation of an yscv oligomer. Molecular Microbiology. 82(2):502-514.

Dohlich K, Zumsteg A, Goosmann C, Kolbe M. 2014. A substrate-fusion protein is trapped inside the type iii secretion system channel in shigella flexneri. Plos Pathogens. 10(1).

Duncan MC, Linington RG, Auerbuch V. 2012. Chemical inhibitors of the type three secretion system: Disarming bacterial pathogens. Antimicrob Agents Chemother. 56(11):5433-5441.

Faudry E, Perdu C, Attrée I. 2013. Pore formation by t3ss translocators: Liposome leakage assay. Methods Mol Biol. 966:173-185.

Felek S, Tsang TM, Krukonis ES. 2010. Three yersinia pestis adhesins facilitate yop delivery to eukaryotic cells and contribute to plague virulence. Infect Immun. 78(10):4134-4150.

Garcia JT, Ferracci F, Jackson MW, Joseph SS, Pattis I, Plano LR, Fischer W, Plano GV. 2006. Measurement of effector protein injection by type iii and type iv secretion systems by using a 13-residue phosphorylatable glycogen synthase kinase tag. Infect Immun. 74(10):5645-5657.

Harmon DE, Davis AJ, Castillo C, Mecsas J. 2010. Identification and characterization of small-molecule inhibitors of yop translocation in yersinia pseudotuberculosis. Antimicrob Agents Chemother. 54(8):3241-3254.

Hu B, Lara-Tejero M, Kong Q, Galán JE, Liu J. 2017. In situ molecular architecture of the salmonella type iii secretion machine. Cell. 168(6):1065-1074.e1010.

Hu B, Morado DR, Margolin W, Rohde JR, Arizmendi O, Picking WL, Picking WD, Liu J. 2015. Visualization of the type iii secretion sorting platform of shigella flexneri. Proc Natl Acad Sci U S A. 112(4):1047-1052.

Kauppi AM, Nordfelth R, Uvell H, Wolf-Watz H, Elofsson M. 2003. Targeting bacterial virulence: Inhibitors of type iii secretion in yersinia. Chem Biol. 10(3):241-249.

Krall R, Zhang Y, Barbieri JT. 2004. Intracellular membrane localization of pseudomonas exos and yersinia yope in mammalian cells. J Biol Chem. 279(4):2747-2753.

Kubori T, Matsushima Y, Nakamura D, Uralil J, Lara-Tejero M, Sukhan A, Galán JE, Aizawa SI. 1998. Supramolecular structure of the salmonella typhimurium type iii protein secretion system. Science. 280(5363):602-605.

Lloyd SA, Norman M, Rosqvist R, Wolf-Watz H. 2001. Yersinia yope is targeted for type iii secretion by n-terminal, not mrna, signals. Mol Microbiol. 39(2):520-531.

Marenne MN, Journet L, Mota LJ, Cornelis GR. 2003. Genetic analysis of the formation of the ysc-yop translocation pore in macrophages by yersinia enterocolitica: Role of lcrv, yscf and yopn. Microb Pathog. 35(6):243-258.

Mattei P, Faudry E, Job V, Izore T, Attree I, Dessen A. 2011. Membrane targeting and pore formation by the type iii secretion system translocon. Febs Journal. 278(3):414-426.

Mehigh RJ, Sample AK, Brubaker RR. 1989. Expression of the low calcium response in yersinia pestis. Microb Pathog. 6(3):203-217.

Miura M, Terajima J, Izumiya H, Mitobe J, Komano T, Watanabe H. 2006. Ospe2 of shigella sonnei is required for the maintenance of cell architecture of bacterium-infected cells. Infect Immun. 74(5):2587-2595.

Morgan JM, Duncan MC, Johnson KS, Diepold A, Lam H, Dupzyk AJ, Martin LR, Wong WR, Armitage JP, Linington RG et al. 2017. Piericidin a1 blocks yersinia ysc type iii secretion system needle assembly. mSphere. 2(1).

Nans A, Kudryashev M, Saibil HR, Hayward RD. 2015. Structure of a bacterial type iii secretion system in contact with a host membrane in situ. Nat Commun. 6:10114.

Pha K, Navarro L. 2016. Yersinia type iii effectors perturb host innate immune responses. World J Biol Chem. 7(1):1-13.

Radics J, Konigsmaier L, Marlovits T. 2014. Structure of a pathogenic type 3 secretion system in action. Nature Structural & Molecular Biology. 21(1):82-+.

Rolsma SL, Frank DW. 2014. In vitro assays to monitor the activity of pseudomonas aeruginosa type iii secreted proteins. Methods Mol Biol. 1149:171-184.

Rosqvist R, Forsberg A, Rimpiläinen M, Bergman T, Wolf-Watz H. 1990. The cytotoxic protein yope of yersinia obstructs the primary host defence. Mol Microbiol. 4(4):657-667.

Sansonetti PJ, Ryter A, Clerc P, Maurelli AT, Mounier J. 1986. Multiplication of shigella flexneri within hela cells: Lysis of the phagocytic vacuole and plasmid-mediated contact hemolysis. Infect Immun. 51(2):461-469.

Schwiesow L, Lam H, Dersch P, Auerbuch V. 2015. Yersinia type iii secretion system master regulator lcrf. J Bacteriol. 198(4):604-614.

Straley SC, Bowmer WS. 1986. Virulence genes regulated at the transcriptional level by ca2+ in yersinia pestis include structural genes for outer membrane proteins. Infect Immun. 51(2):445-454.

Tree JJ, Wang D, McInally C, Mahajan A, Layton A, Houghton I, Elofsson M, Stevens MP, Gally DL, Roe AJ. 2009. Characterization of the effects of salicylidene acylhydrazide compounds on type iii secretion in escherichia coli o157:H7. Infect Immun. 77(10):4209-4220.

Troisfontaines P, Cornelis G. 2005. Type iii secretion: More systems than you think. Physiology. 20:326-339.

Trülzsch K, Roggenkamp A, Aepfelbacher M, Wilharm G, Ruckdeschel K, Heesemann J. 2003. Analysis of chaperone-dependent yop secretion/translocation and effector function using a mini-virulence plasmid of yersinia enterocolitica. Int J Med Microbiol. 293(2-3):167-177.

Wang H, Avican K, Fahlgren A, Erttmann SF, Nuss AM, Dersch P, Fallman M, Edgren T, Wolf-Watz H. 2016. Increased plasmid copy number is essential for yersinia t3ss function and virulence. Science. 353(6298):492-495.

Wang Y, Sun M, Bao H, Zhang Q, Guo D. 2013. Effective identification of bacterial type iii secretion signals using joint element features. PLoS One. 8(4):e59754.

CHAPTER 2

An experimental pipeline for initial characterization of bacterial type III secretion system inhibitor mode of action using enteropathogenic *Yersinia*

By: Jessica Morgan, Jocelyn Delgado, Hanh Lam, Justin Luu, Sina Mohammadi, Ralph R. Isberg, Helen Wang, and Victoria Auerbuch

ABSTRACT

Dozens of Gram negative pathogens use one or more type III secretion systems (T3SS) to disarm host defenses or occupy a beneficial niche during infection of a host organism. While the T3SS represents an attractive drug target and dozens of compounds with T3SS inhibitory activity have been identified, few T3SS inhibitors have been validated and mode of action determined. One issue is the lack of standardized orthogonal assays following high throughput screening. Using a training set of compounds previously shown to possess T3SS inhibitory activity, we demonstrate the utility of an experiment pipeline comprised of five distinct assays to assess the stages of type III secretion impacted: T3SS gene expression, T3SS basal body and needle assembly, secretion of cargo through the T3SS, and translocation of T3SS effector proteins into host cells. We used enteropathogenic *Yersinia* as the workhorse T3SS-expressing model organisms for this experimental pipeline. We find that this experimental pipeline is capable of rapidly distinguishing between T3SS inhibitors that interrupt the process of type III secretion at different points in T3SS assembly and function. For example, our data suggests that C3, a malic diamide, blocks either activity of the assembled T3SS or alters the structure of the T3SS in a way that blocks T3SS cargo secretion but not antibody recognition of the T3SS needle. In contrast, our data predicts that C4, a haloid-containing sulfonamidobenzamide, disrupts T3SS needle subunit secretion or assembly. Furthermore, our data suggests that misregulation of copy number control of the pYV virulence plasmid, which encodes the *Yersinia* T3SS, should be considered as a

possible mode of action for compounds with T3SS inhibitory activity.

INTRODUCTION

The type III secretion system (T3SS) is a macromolecular nanosyringe used by dozens of Gram negative pathogens, including *Yersinia*, *Shigella*, *Salmonella*, *Chlamydia* and *Pseudomonas*, to inject effector proteins into target host cells (Deng et al. 2017). The core structure of the T3SS consists of a basal body that anchors the entire complex in the bacterial membrane and assembles first. The basal body is composed of three proteins, which oligomerize into rings. SctD and SctJ form two rings in the bacterial inner membrane (IM) and SctC, a member of the secretin family of proteins, forms a ring in the bacterial outer membrane (OM)(Bergeron et al. 2013). These three rings are connected in the center by a hollow inner rod and the IM rings are closely associated with the SctN ATPase complex whose integrity is essential to the T3SS (Diepold et al. 2010). In addition to ATP, the proton motive force is also important for T3SS activity (Wilharm et al. 2004), although how the T3SS harnesses the proton motive force remains unclear. Once active, the basal body secretes the SctF needle protein, which polymerizes into a straight, hollow tube protruding into the extracellular space. In *Yersinia* species pathogenic to mammals, the fully assembled Ysc T3SS needle is composed of ~140 SctF subunits, is 65 nm in length, and harbors a tip complex composed of a pentamer of the hydrophilic LcrV translocator protein (Broz et al. 2007). Upon host cell contact, two additional hydrophobic translocator proteins, YopD and YopB, are secreted through the Ysc

needle to form a translocon complex that causes pore formation in the host membrane, facilitating the translocation of effector proteins to the host cytoplasm (Büttner and Bonas 2002).

The *Yersinia* Ysc T3SS is highly regulated at the transcriptional, translational, and post-translational levels (Francis et al. 2002; Heroven et al. 2012). The transcription factor LcrF directs transcription of genes encoding the T3SS structural, regulatory, and effector proteins, all of which are encoded on the 70 kb pYV virulence plasmid (Schwiesow et al. 2015). Several factors govern regulation of LcrF expression, including temperature and the transcription factor IscR (Miller et al. 2014). Importantly, pYV copy number increases during active type III secretion, and this is important for *Yersinia* virulence (Wang et al. 2016). In addition, the T3SS functions on a regulatory feedback loop in which active secretion leads to upregulated transcription of T3SS genes (Cornelis et al. 1987; Francis et al. 2002), although the mechanism behind this remains unclear.

A number of pathogens require one or more T3SSs for virulence, as genetic ablation causes attenuation in animal models and clinical isolates harbor plasmids or pathogenicity islands that encode T3SS genes (Coburn et al. 2007). An antibody against the *Pseudomonas aeruginosa* T3SS needle tip protein PcrV is part of a current Phase II clinical trial to treat nosocomial ventilator-associated pneumonia (NCT02696902), indicating that antibodies targeting the T3SS may be used as

therapeutics. However, antibodies have low oral bioavailability and must be administered by injection; small molecules with high oral bioavailability are more attractive as therapeutic agents. A number of putative small molecule T3SS inhibitors have been identified in the past 15 years (Anantharajah et al. 2017; Duncan et al. 2012; Marshall and Finlay 2014), yet only one class of compounds can be considered validated. Almost all published T3SS inhibitors have off target effects that may underlie their T3SS disruption. For example, the best studied class of T3SS inhibitors, the salicylidene acylhydrazides, are thought to cause deregulation of T3SS genes through an unknown mechanism, yet the activity of some salicylidene acylhydrazides is dependent on iron chelation (Beckham and Roe 2014). The phenoxyacetamides represent the only class of compounds that inhibit the T3SS in a physiologically relevant cellular context, protect against a bacterial infection (*P. aeruginosa* abscess formation in mice), and have a validated molecular target, the SctF needle subunit (Berube et al. 2017; Bowlin et al. 2014).

We have developed a series of assays that can be employed to determine initial mode of action for compounds with T3SS inhibitory activity. We chose to use the enteropathogens *Yersinia pseudotuberculosis* and *Yersinia enterocolitica* as the workhorses for this assay pipeline because of the number of inhibitors discovered using *Yersinia* as the screening organism as well as the wealth of genetic and biochemical tools available. Importantly, the assays selected had to be amenable to miniaturization, as compound availability is often limiting. Since interfering with

T3SS gene expression, basal body assembly, needle assembly, and host cell effector protein translocation individually could lead to inhibition of T3SS activity, we designed our assay pipeline to measure each of these stages of type III secretion. Inhibitors of LcrF and its homolog ExsA from *Pseudomonas aeruginosa* have been described (Marsden et al. 2016). In addition, it is possible that a small molecule with T3SS inhibitory activity could exert its effect by inhibiting secretion-associated increase of pYV copy number, leading to a decrease in T3SS gene expression. Therefore, two pipeline assays measure pYV copy number and T3SS gene expression. Once T3SS genes are expressed, the T3SS basal body assembles followed by the T3SS needle. Two additional pipeline assays measure SctD (YscD in *Yersinia*) localization to the inner membrane and SctF (YscF) needle assembly. The last pipeline assay monitors efficiency of T3SS effector protein (Yop) translocation into target host cells.

MATERIALS AND METHODS

Compounds and antibodies. Compound 3 (CAS# 443329-02-0), compound 4 (CAS# 138323-28-1), and INP0007 (CAS# 300668-15-9) were obtained from Chembridge. INP0010 (CAS# 68639-26-9) was obtained from ChemDiv. Compound 20 (CAS# 489402-27-9) was obtained from TimTek. The anti-YscF antibody was raised in rabbits against the *Y. pseudotuberculosis* YscF peptide KDKPDNPALLADLQH (Morgan et al. 2017).

Bacterial Strains and Growth Conditions. Bacterial strains used in this paper are listed in Table 2. *Y. pseudotuberculosis* (IP2666) and *Y. enterocilitica* (E40) were grown, unless otherwise specified, in 2xYT (yeast extract-tryptone) at 26°C shaking overnight. The cultures were back-diluted into low calcium media (2xYT plus 20 mM sodium oxalate and 20 mM $MgCl_2$) to an optical density (OD_{600}) of 0.2 and grown for 1.5 hours at 26°C shaking followed by 1.5 hours at 37˚C to induce Yop synthesis as previously described (Auerbuch et al. 2009).

Strain	**Description**	**Reference**
Wild type	*Y. pseudotuberculosis* IP2666, naturally lacking YopT expression	Bliska et al 1991
Δyop6 + pYopM-Bla	*Y. pseudotuberculosis* IP2666 Δ*yopHEMOJ* pYopM-Bla	Duncan 2014
Δyop6/Δ*yop*B + pYopM-Bla	*Y. pseudotuberculosis* IP2666 Δ*yopHEMOJ* pYopM-Bla	Duncan 2014
pYV40-EGFP-*yscD*	*Y. enterocolitica* serotype O9 strain E40	Diepold 2010
Wild type	*Y. enterocolitica* 8081 serotype O8	Portnoy et al. 1981
YpIII/pIBX	*Y. pseudotuberculosis* YpIII with Tn5*luxCDABE* inserted in the Tn1000 resolvase homolog in pCD1 (wild type); Km^r	Caliper Life Sciences (Fahlgran)

YpIII/(pIBX)$_{n=1}$	*Y. pseudotuberculosis* YpIII/pIBX derivative with the pIBX virulence plasmid lacking 3426 bp encoding the IncFII replicon and R6K suicide plasmid, integrated into YPK_3687 in the chromosome; Km^r, Cm^r	Wang 2016 Miller 1988
p*yop*H FLAG mCherry	*Y. pseudotuberculosis* IP2666 containing the *yopH* promoter and YopH with an N-terminal FLAG tag and a C-terminal ssrA-tagged mCherry cloned into pMMB67EH	This study
flhDC$^{Y.pestis}$	*Y. pseudotuberculosis* Δ*yopHEMOJ/flhDC*$^{Y. pestis}$	Auerbuch et al 2009

Table 2. Bacterial strains used in this study.

Construction of YopH transcriptional reporter. An expression cassette containing the yopH promoter and FLAG (5' terminus)- and ssrA (3' terminus)-tagged mCherry was generated using SOE PCR and cloned into pMMB67EH (Horton et al. 1990; Karzai et al. 2000; Pettersson et al. 1996). The *yopH* promoter was amplified from pHYopT (gift from J. Bliska) using oligonucleotides 425 and 426 (Table 3). mCherry (gift from R. Tsien) was amplified using oligonucleotides 427 and 431. FLAG and ssrA sequences were incorporated into oligonucleotides 426/427 and 431 respectively. Oligonucleotides 425 and 431 were used to generate the PyopH-FLAG-mCherry-ssrA cassette. PCR product was digested with BamHI and EcoRI and cloned into similarly digested pMMB67EH. Site directed mutagenesis using oligonucleotides 437 and 438 was used to generate the AAV variant of the ssrA tag.

Number	Sequence	Dir	Function	Enzyme
SMP425	GGAggatccGCTGCGCGATGTACTGACCCG	>>	pyopH 5'	BamHI
SMP426	CTCCTCGCCCTTGCTCACCATCTTGTCATCGTCGTCCTTGTAATCCATATGTCCCTCCTTAATTAAATACACGCCTATAC	<<	pyopH-FLAG-mCherry/EGFP (for SOE, 3', use with SMP425)	
SMP427	GTATAGGCGTGTATTTAATTAAGGAGGGACATatggattacaaggacgacgatgacaagAtggtgagcaagggcgaggag	>>	pyopH-FLAG-mCherry/EGFP (for SOE, 5', use with SMP428)	
SMP428	GAAgaattcTTACTTGTACAGCTCGTCCATGCCG	<<	mCherry/EGFP 3'	EcoRI
SMP431	GAAgaattcTTACGCTGCTAACGCGTAATTCTCATCATTCGCTGCCTTGTACAGCTCGTCCATGCCGC	<<	mCherry/EGFP 3' with ssrA (LAA) tag (use with 425,427)	EcoRI
SMP435	CAGCGAATGATGAGAATTACGCGTTAGtAGCGTAAgaattctgtttcctgtgtg	>>	LAA->LVA mut. for pMMB67EH-PyopH-FLAG-mCherry (top)	
SMP436	CACACAGGAAACAGAATTCTTACGCTACTAACGCGTAATTCTCATCATTCGCTG	<<	LAA->LVA mut. for pMMB67EH-pyopH-FLAG-mCherry (bottom)	

SMP437	GCAGCGAATGATGAGAATTACGCGgcAGCAGtGTAAgaattctgttcctgtgtgaaattg	>>	LAA->AAV mut. for pMMB67EH-pyopH-FLAG-mCherry (top)	
SMP438	CAATTTCACACAGGAAACAGAATTCTTACACTGCTGCCGCGTAATTCTCATCATTCGCTGC	<<	LAA->AAV mut. for pMMB67EH-PyopH-FLAG-mCherry (bottom)	
SMP455	CAAGGCAGCGAATGATGAGAATTACGCGgcAtCAGtGTAAGAATTCtgtttcctgtgtgaaattgttatc	>>	LAA->ASV mut. for pMMB67EH-pyopH-FLAG-mCherry (top)	
SMP456	GATAACAATTTCACACAGGAAACAGAATTCTTACACTGATGCCGCGTAATTCTCATCATTCGCTGCCTTG	<<	LAA->ASV mut. for pMMB67EH-pyopH-FLAG-mCherry (bottom)	

Table 3. Oligonucleotides used to generate pYopH FLAG mCherry.

Type III secretion assay. Visualization of *Y. pseudotuberculosis* T3SS cargo secreted in broth culture was performed as previously described (Auerbuch et al. 2009). *Y. pseudotuberculosis* low calcium media cultures were grown for 1.5 hrs at 26°C. Compounds or DMSO were added and the cultures were switched to 37°C for another 2 hrs. DMSO concentration did not exceed 0.2%. Post incubation, cultures were spun down at 21.1 rcf for 10 min at room temperature. Supernatants were transferred to a new eppendorf tube. Ten percent final trichloroacetic acid (TCA) was added and the mixture vortexed vigorously. Samples were incubated on ice for 20 min and then spun down at 21.1 rcf for 15 min at 4°C. The pellet was resuspended

in final sample buffer (FSB) + 20% DTT. Samples were boiled for 15 min prior to running on a 12.5% SDS-PAGE gel. Sample loading was normalized for bacterial density (OD_{600}) of each sample. *Y. pseudotuberculosis* samples were visualized with coomassie blue staining. Densitometric quantification of the bands was done using Image Lab software (Bio-Rad), setting the relevant DMSO-treated *Y. pseudotuberculosis* YopE band to 1.00.

Quantitative Real-time PCR. Overnight bacterial cultures grown in 2xYT were back-diluted and grown in Low calcium media (2xYT plus 20 mM sodium oxalate and 20 mM $MgCl_{2)}$ at 37˚C to induce type III secretion, in the presence of DMSO or other compounds as indicated. Compounds were added at indicated concentrations or the equivalent volumes of DMSO were added and the cultures switched to 37°C for another 3 hrs. DMSO concentration did not exceed 0.2%. RNA was isolated using an RNeasy Plus Micro Kit (Qiagen) according to the manufacturer's instructions. SYBR Green PCR master mix (Applied Biosystems) was used for qPCR reactions according to the manufacturer's instructions and a 60°C annealing temperature. Primers used are listed in Table 4. Results were analyzed using the Bio-Rad CFX software.

Name	**Sequence**	**Reference**
FqyopE	CCATAAACCGGTGGTGAC	(Morgan et al. 2017)
RqyopE	CTTGGCATTGAGTGATACTG	(Morgan et al. 2017)
FqyscN	CTTCGCTTATTCGTAGTGCT	(Miller et al. 2014)
RqyscN	TCGCCTAAATCAGACTCAAT	(Miller et al. 2014)
Fq16s	AGCCAGCGGACCACATAAAG	(Merriam et al. 1997)

Rq16s	AGTTGCAGACTCCAATCCGG	(Merriam et al. 1997)
FqyscF	TCTCTGGATTTACGAAAGGA	(Miller et al. 2014)
RqyscF	GCTTATCTTTCAATGCTGCT	(Miller et al. 2014)
FqlcrF	GGAGTGATTTTCCGTCAGTA	(Miller et al. 2014)
RqlcrF	CTCCATAAATTTTTGCAACC	(Miller et al. 2014)
FqyscD	TGCCAGAGACGTTACAGGTT	This study
RqyscD	CATCCTGGTTATACTCGCGC	This study
FqErpA	TACCGGTGGTGGATGTAGCGGG	(Miller et al. 2014)
RqErpA	ATAATCCACGGCACCGCCCAC	(Miller et al. 2014)
FqyopK	ATGTTGCCATTCGTATAAGC	This study
RqyopK	GAGAACGGATGTTTGTTCAT	This study
FqyopH	ACACTACAAGACGCCAAAG	This study
RqyopH	GTGAAGGGCTGAATGTGAA	This study
FqlcrV	TGATATCGAATTGCTCAAGA	This study
RqlcrV	CGGCGGTTAAAGAGAAAT	This study
FqL9	TGGGTGACCAAGTCAACGTA	This study
RqL9	GTCGCGAGTACCGATAGAGC	This study

Table 4. qPCR primers used in this study.

YopH Transcriptional reporter assay. Overnight bacterial cultures grown in 2xYT were back-diluted and grown in Low calcium media (2xYT plus 20 mM sodium oxalate and 20 mM $MgCl_2$) for 1.5 hours at 26°C shaking, and were then shifted to 37˚C to induce type III secretion, in the presence of DMSO or other compounds as indicated, for 3 hours. DMSO concentration does not exceed 0.2%. 200 µl of cells were then spun down at 3.5 rcf for five minutes, resuspended in 200 µl 1x PBS, and mCherry fluorescence and optical density measured in a black, clear bottom 96 well plate (costar) on a Perkin Elmer Victor X3 plate reader.

Immunofluorescence staining of YscF. As described previously (Morgan et al. 2017) **.** Cultures were grown overnight in 2xYT. Cultures were back diluted to an OD_{600} of 0.2 and grown, shaking, at 26˚C for 1.5 hours. Compounds were added at indicated concentrations or the equivalent volume of DMSO was added and the

cultures switched to 37°C for another 3 hrs. DMSO concentration did not exceed 0.2%. Bacteria were fixed by the addition of a mix of 800 µl 4% paraformaldehyde, 1 µl 25% glutaraldehyde, and 40 µl 0.5 M $NaPO_4$ pH 7.4 to 500 µl of the bacterial culture for 15 min at RT followed by 30 min or longer on ice. Fixed bacteria were gently sedimented (5000 × g for 5 min), washed 4 times with PBS and stored in 250 mM glucose, 10 mM Tris-HCl pH 7.5, and 1 mM EDTA. 8 µL of the fixed cells were added to coverslips and allowed to set until just dried. Coverslips were blocked overnight with PBST + 3% BSA (PBST/BSA) at 4°C. Blocking solution was removed and anti-YscF primary antibody was added at 1:10,000 in PBST/BSA and rocked at 4°C for 4 hours. Coverslips were carefully rinsed in ice cold PBST + 0.1% Tween-20 several times and incubated with Alexa fluor 594 or 488 anti-rabbit secondary antibody (Invitrogen) at 1:10,000 in PBST/BSA and rocked at 4°C for 3 hours followed by rinsing again in ice cold PBST + 0.1% Tween-20 several times. Coverslips were then stained for nuclear material with Hoechst 33342 (Thermo Scientific) at 1:10,000 in PBST/BSA and left in the dark at RT for 30 minutes. Coverslips were washed in ice cold PBST + 0.1% Tween-20 several times, allowed to dry briefly, mounted onto glass coverslips with Prolong Gold (Thermo Scientific), and sealed with clear nail polish. Images were taken with the Zeiss Axioimager Z2 widefield microscope under 63x/1.4 oil immersion using Zen software, pseudocolored, and merged in FIJI. YscF puncta were counted using IMARIS software.

YscD analysis. *Y. enterocolitica* expressing EGFP-YscD were grown overnight in brain heart infusion (BHI) broth containing nalidixic acid (35 μg/ml) and diaminopimelic acid (80 μg/ml) (Diepold et al. 2010). Overnight cultures were backdiluted to an optical density of 0.2 in M9 minimal medium supplemented with casamino acids. Cultures were grown for 1.5 hrs at 26°C. Compounds were added at indicated concentrations or the equivalent volumes of DMSO were added and the cultures switched to 37°C for another 3 hrs. DMSO concentration did not exceed 0.2%. 2 μl of culture were layered on a patch of 1% agarose in water (Skinner et al. 2013) supplemented with 80 μg/ml diaminopimelic acid, 5mM EDTA, 10mM $MgCl_2$, and either compounds at indicated concentrations or the equivalent volume of DMSO (Diepold et al. 2010). Images were taken with a Zeiss Axioimager Z2 widefield microscope under 63x/1.4 oil immersion using Zen software, pseudocolored, and merged in FIJI. YscF puncta were counted using IMARIS software.

pYV copy number. *Y. pseudotuberculosis* YpIII/pIBX$_{N=1}$ and YpIII/pIBX were grown overnight in 2xYT media containing Kanamycin (30 μg/ml). Overnight cultures were backdiluted to an optical density of 0.2 in M9 supplemented with casamino acids. Cultures were grown for 1.5 hrs at 26°C. Compounds were added at indicated concentrations or the equivalent volumes of DMSO were added and the cultures switched to 37°C for another 3 hrs. DMSO concentration did not exceed 0.2%. 200 μl of each respective culture was added to a clear bottom, black 96 well plate (costar) and was then read for both optical density and luminescence on the

Perkin Elmer Victor X3 plate reader.

YopM translocation assay. Translocation of the YopM-β-lactamase (YopM-Bla) reporter effector protein was carried out as previously described (Duncan et al. 2012). A total of $6x10^3$ CHO-K1 cells were plated in each well of a 384-well plate in 50 µl of F-12K medium plus 10% FBS and 1% glutamine and incubated overnight. The following day, *Y. pseudotuberculosis* YopM-Bla overnight cultures were back diluted into low-calcium 2xYT medium to an OD_{600} of 0.2 and grown in a shaking incubator at 26°C for 1.5 h. Compounds were added at indicated concentrations or the equivalent volumes of DMSO were added and the cultures switched to 37°C for another 3 hrs. DMSO concentration did not exceed 0.2%. Immediately prior to infection, the F-12K media was removed and replaced with RPMI plus 10% FBS and compounds or DMSO were also added to the 384-well plate containing CHO-K1 cells. *Y. pseudotuberculosis* were then added to the CHO-K1 plate at an MOI of 7. Five minutes after this transfer, the plate was centrifuged at 290 × g for 5 min to initiate bacterium-host cell contact and incubated for 1 h at 37°C and 5% CO_2. Thirty minutes prior to the end of the infection, CCF2-AM (Invitrogen) was added to each well, and the plate covered in foil and incubated at room temperature. At the end of the infection, the medium was aspirated and fresh 4% paraformaldehyde added to each well for 20 min to fix the cells. The paraformaldehyde was then aspirated and the DNA dye DRAQ5 (Cell Signaling Technology) in PBS was added to each well. The monolayers were incubated at room temperature for 10 min, washed once with

PBS, and visualized using an ImageXpress^{MICRO} automated microscope and MetaXpress analysis software (Molecular Devices). The number of YopM-Bla-positive cells was calculated by dividing the number of blue (CCF2-cleaved) cells by the number of green (total CCF2) cells. Data from three separate wells were averaged for each experiment.

Growth curves. Overnight cultures of wild-type (WT) *Y. pseudotuberculosis* IP2666 were back diluted to an OD_{600} of 0.1, and 200 µl was added to each well of a 96-well plate. Compounds were added at their indicated concentrations, not exceeding 0.2% DMSO, or kanamycin at 50 µg/ml. Bacteria were grown at 26°C in 2xYT medium and the OD_{600} of the culture was measured every hour for 13 h using a VersaMax Tunable Microplate Reader (Molecular Devices). The 96-well plates were intermittently shaken throughout the experiment.

Motility assay. Following overnight growth one microliter of WT *Y. pseudotuberculosis* or a non-motile mutant expressing *flhDC*$^{Y.\ pestis}$ (Auerbuch et al. 2009)was spotted onto motility medium containing either 1% tryptone, 0.25% agar or either 1% tryptone, 0.25% agar supplemented with 5 mM EGTA, 20 mM $MgCl_2$ in six-well plates. Each well contained either 0.3% DMSO or 50 µM INP0007 or INP0010. The plates were stored at 26°C for 24 h before the diameter of swimming motility was measured.

RESULTS

T3SS inhibitor training set for assay pipeline

We selected a training set of commercially-available compounds to validate our assay pipeline (Table 1). All compounds selected met two strict requirements: demonstrated inhibitory activity on the T3SS and absence of bactericidal activity within six hours to accommodate the timeframe of the pipeline assays (Figure 1A-C).

Compound name	Chemical Structure	Shown to inhibit:	References
Compound 3 (CAS: 443329-02-0)	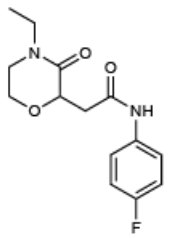	-Inhibition of ExoS-Bla and YopE-Bla secretion in *Pseudomonas* and *Yersinia*, respectively	Aiello et al. 2010
Compound 4 (CAS: 138323-28-1)	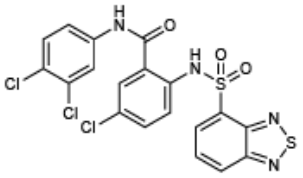	-Inhibition of T3SS gene expression and effector secretion in *Yersinia*	Kauppi et al. 2003
INP0007 (CAS: 300668-15-9)	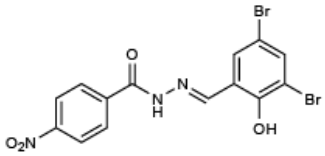	-Inhibition of T3SS gene expression, effector secretion, and motility in *Yersinia* -Inhibition of T3SS (SPI1) gene expression, secretion, and translocation in *Salmonella*	Kauppi et al. 2003 Nordfelth et al. 2005 Negrea et a. 2007
INP0010 (CAS: 68639-26-9)	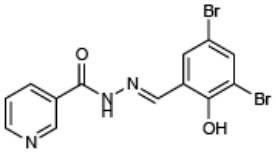	-Inhibition of T3SS gene expression and effector secretion in *Yersinia* -Inhibition of T3SS gene expression, secretion, and	Nordfelth et al. 2005 Negrea et al. 2007 Tree et al. 2009

		invasion in *Salmonella* -Inhibition of virulence genes, including the T3SS in *E. coli*	
Compound 20 (CAS: 489402-27-9)	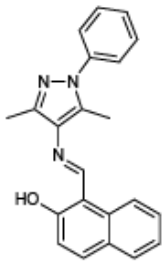	-Inhibition of T3SS dependent effector translocation in *Yersinia*	Harmon et al. 2010

Table 1. Compounds used in this study and their reported activity.

Compound 4 (C4), a haloid-containing sulfonamidobenzamide, was identified through a luciferase-based T3SS gene promoter fusion screen and a potent inhibitor of T3SS gene expression (Kauppi et al. 2003). We chose this compound because it was shown, albeit modestly, to inhibit expression of the LcrF master regulator of the T3SS in *Yersinia* (Kauppi et al. 2003) and we therefore expected that it would have a broad impact on all stages of type III secretion downstream of T3SS expression in our assay pipeline. From the same high throughput screening strategy that identified C4, two members of the salicylidene acylhydrazide class of inhibitors, INP0007 (Kauppi et al. 2003) and INP0010 (Nordfelth et al. 2005), were identified. Despite a large number of studies, the mechanism of action of these compounds remains unclear and there is evidence of off target effects on global virulence gene expression by at least

some salicylidene acylhydrazides (Tree et al. 2009). In fact, INP0010 decreased *Yersinia* growth starting seven hours after initiation of treatment (Fig. 1D), consistent with previous reports (Veenendaal et al. 2009). Compound 3 (C3), a malic diamide, was shown to inhibit ExoS secretion in *Pseudomonas aeruginosa* and YopE secretion in *Yersinia pestis* (Aiello et al. 2010). This compound is structurally related to another class of T3SS inhibitors, the phenoxyacetamides, which were proposed to target the PscF needle subunit in *Pseudomonas* (Bowlin et al. 2014). This compound was expected to disrupt T3SS needle assembly without impacting T3SS gene expression. Compound 20 (C20) was identified in a T3SS effector protein-β-lactamase reporter translocation screen, but had no significant effect on the ability of the bacteria to secrete T3SS effectors in the absence of host cells, pointing to the possibility that this compound specifically blocks the bacteria-host cell interaction (Harmon et al. 2010). Therefore, C20 was expected to inhibit the translocation of effector proteins into host cells but not impact T3SS gene expression and assembly.

An advantage of using Ysc-expressing *Yersinia* for our assay pipeline is that removing calcium from the culture medium enables T3SS effector proteins to be secreted into the supernatant in the absence host cells (Forsberg and Wolf-Watz 1988; Mehigh et al. 1989; Perry et al. 1986; Sample et al. 1987; Straley and Bowmer 1986; Yother and Goguen 1985), providing a useful method of monitoring efficiency of T3SS inhibition. As expected, all test compounds except C20 exhibited significant inhibition of effector Yop secretion (Figure 1AB). Importantly, this secretion assay

was used routinely to ensure the efficacy of each batch of compound purchased and after one month in storage. Therefore, even when a compound had no effect in a particular assay, we could be confident that it was still active as a T3SS inhibitor.

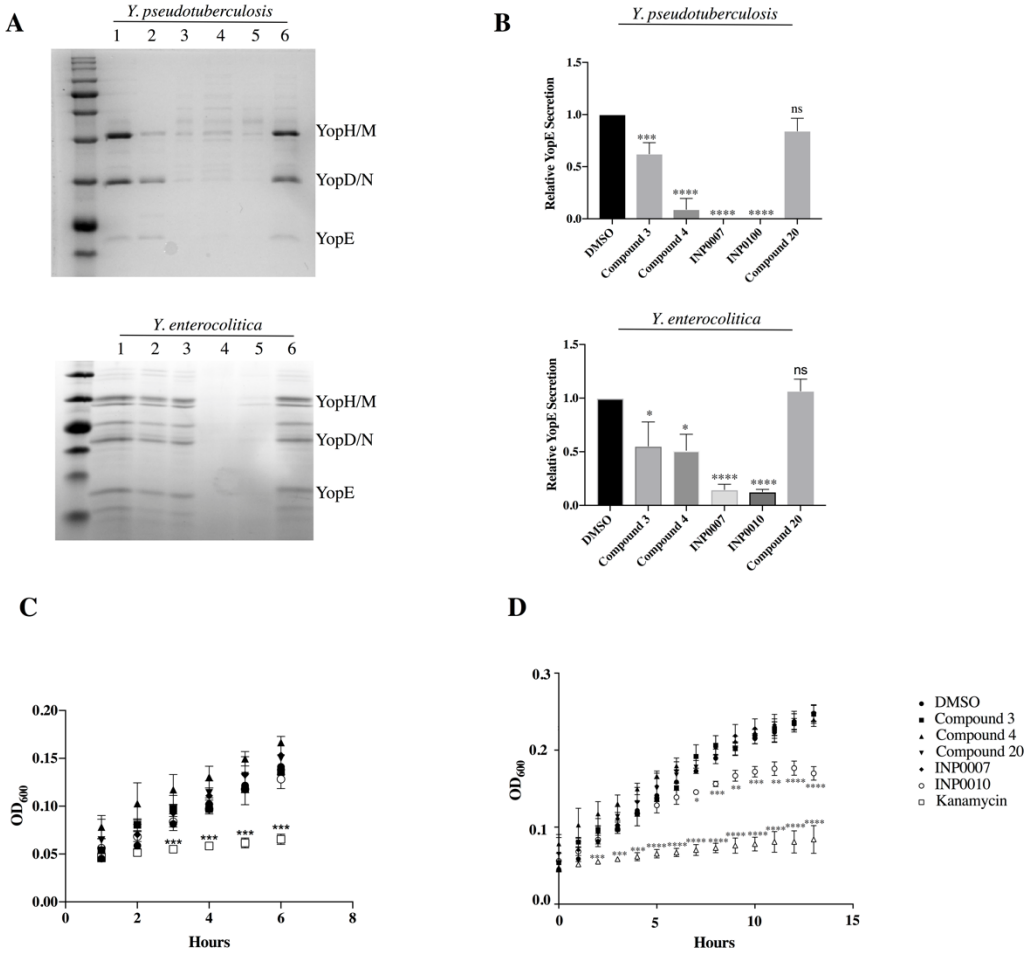

Figure 1. Efficiency of T3SS effector protein secretion and bacterial growth in the presence of T3SS inhibitors. **(A-B)** The relative efficiency of effector protein secretion into the culture supernatant was analyzed following bacterial growth under T3SS-inducing conditions in the presence of either 50 µM compound or equivalent volume of DMSO. **(A)** The secretome of *Y. pseudotuberculosis* IP2666 and *Y. enterocolitica* 8081 was precipitated with trichloroacetic acid, separated by SDS-PAGE, and visualized by staining with Coomassie blue. (1) DMSO (2) Compound 3 (3) Compound 4 (4) INP0007 (5) INP0010 (6) Compound 20. **(B)** Quantification of the YopE protein band by densitometry relative to the DMSO control. The average of 3 (*Y. pseudotuberculosis*) or 4 (*Y. enterocolitica*) biological replicates ± standard deviation is shown. **(C-D)** *Y. pseudotuberculosis* growth at 26°C in the presence of 50

μM compound or DMSO was tracked by measuring optical density. The average of 3 biological replicates ± standard deviation is shown. ****, P < 0.0001; ***, P= 0.0006 (one way ANOVA with Bonferroni post hoc test).

Assessment of T3SS gene expression

We reasoned that inhibition of the pYV copy number upregulation that occurs during normal induction of type III secretion in *Yersinia* may impact T3SS gene expression, and therefore affect overall T3SS activity. To test this, we employed a *Y. pseudotuberculosis* strain with a luciferase reporter gene cluster integrated onto the pYV virulence plasmid (YpIII/pIBX)

(Fahlgren et al. 2014). As a negative control, we used a strain in which a replication deficient copy of the virulence plasmid as well as the luciferase gene cluster was integrated into the chromosome (referred to as YpIII/pIBX$_{N=1}$)(Wang et al. 2016). In this YpIII/pIBX$_{N=1}$ strain, the ratio of T3SS and luciferase reporter genes versus chromosomal genes remains constant even upon induction of type III secretion (Wang et al. 2016). As expected, expression of *lcrF*, the effector protein *yopE*, the integral inner membrane ring protein *yscD*, and the needle subunit *yscF* were significantly decreased in the YpIII/pIBX$_{N=1}$ strain compared to the YpIII/pIBX strain (Figure 2A). While these data demonstrate that inhibition of pYV gene copy number could impact pYV gene expression, four of the five compounds in our training set did not significantly affect virulence plasmid copy number as measured by luciferase activity, while INP0007 slightly increased copy number (p=0.0054; Figure 2B). In contrast, luciferase expression could be inhibited by blocking general transcription or translation using rifampicin or chloramphenicol (Figure 2B). Therefore, while

inhibiting pYV copy number in *Yersinia* causes a decrease in T3SS activity, we conclude that none of the compounds in our training set act by inhibiting upregulation of pYV copy number.

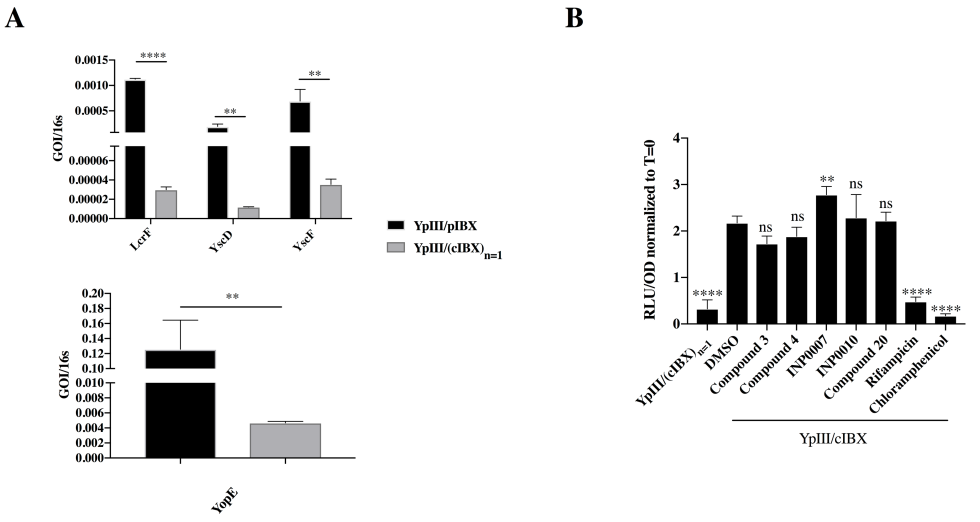

Figure 2. Correlation between pYV copy number and T3SS gene expression. (A) *Y. pseudotuberculosis* encoding luciferase genes on pYV (YPIII/pIBX) or a strain in which pYV-encoded T3SS and luciferase genes were incorporated into the chromosome in single copy (YPIII/(cIBX)$_{n=1}$) were grown for three hours under T3SS-inducing conditions in 50 µM compound or equivalent volume of DMSO and T3SS gene expression evaluated by qPCR. The average of X biological replicates ± standard deviation is shown. **** P<0.0001, **P<0.008 (Student T test). **(B)** *Y. pseudotuberculosis* YpIII/pIBX and YPIII/(cIBX)$_{n=1}$ were grown under T3SS-inducing conditions for three hours in 50 µM compound or equivalent volume of DMSO and luminescence measured as a readout of pYV gene copy number. The average of X biological replicates ± standard deviation is shown. ****, P < 0.0001; ** P=0.0054; * P=0.0334 (one way ANOVA with Bonferroni post hoc test).

In order to determine if the training set compounds negatively impacted T3SS gene expression, we used a *Yersinia* reporter strain containing an unstable YopH-mCherry-AAV transcriptional reporter (Andersen et al. 1998). As expected, C4, INP0007, and

INP0010 inhibited YopH-mCherry-AAV expression when T3SS activity was induced by incubation in low calcium medium at 37˚C (Figure 3A). In order to validate and extend these results, we measured transcript levels of T3SS and non-T3SS genes by qPCR. As expected, C3 and C20 had no significant impact on gene expression (Figure 4). However, under T3SS-inducing low calcium conditions, C4 inhibited expression of all T3SS genes tested, but did not impact expression of two non-T3SS-associated genes: the iron sulfur cluster loading protein *erpA* and the small ribosomal subunit L9. Interestingly, INP0007 and INP0010 significantly inhibited transcript levels of *lcrF*, the needle tip subunit *lcrV*, and effector proteins *yopH*, *yopE*, and *yopK*, but did not inhibit expression of the ATPase *yscN*, *yscF*, and *yscD* under these conditions (Figure 4). To test whether inhibition of secretion via the positive feedback look indirectly inhibits T3SS gene expression, we measured YopH-mCherry fluorescence and *yscD* mRNA levels via qPCR during growth at 37˚C in high calcium (Figure 3BC). Under these conditions, *Yersinia* can assemble the T3SS (Diepold et al. 2010), but no secretion of Yop effectors occurs (Forsberg and Wolf-Watz 1988). C4, INP0007, and INP0010 did not significantly inhibit T3SS gene expression under these conditions, suggesting an indirect effect on T3SS gene expression through inhibition of secretion. While overall expression levels of YscD and YopH are lower in high calcium compared to low calcium conditions, C4, INP0007, and INP0010 did not significantly decrease mCherry fluorescence in high calcium conditions (Figure 3B). Likewise, *yscD* levels were not decreased by C4 in high calcium (Figure 3C). However, *yscD* expression was significantly lower in the Δ*lcrF* mutant compared to

WT under high calcium conditions in the absence of compound. These data indicate that C4 is not likely to target LcrF activity, as *yscD* is predicted to be under LcrF control (Schwiesow et al. 2015).

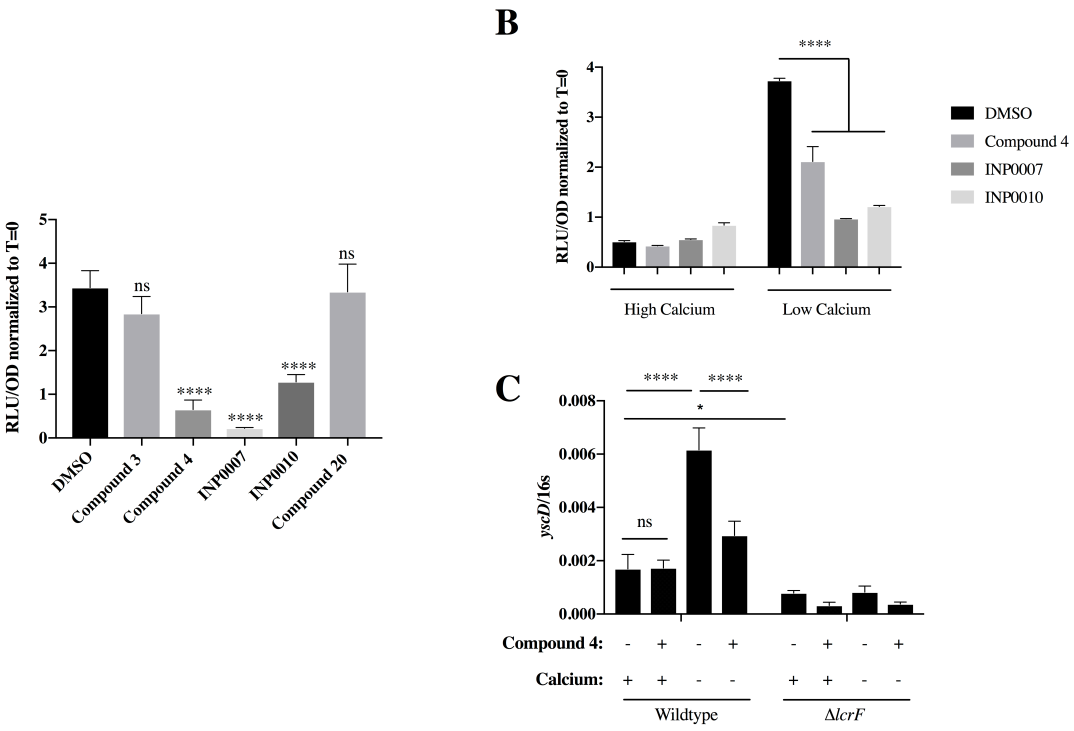

Figure 3. Analysis of *yopH*-mCherry fluorescence to assess T3SS gene expression. (A-B) *Y. pseudotuberculosis* p*yopH* FLAG mCherry was grown under T3SS-inducing (A; B, low calcium) or non-inducing (B, high calcium) conditions and mCherry fluorescence measured at three hours after addition of 50 µM compound or equivalent volume of DMSO. **(C)** *Y. pseudotuberculosis* wildtype or Δ*lcrF* were grown in low or high calcium media for three hours in 50 µM C4 or equivalent volume of DMSO and *yscD* mRNA levels measured by qPCR. ****P<0.0001 (one way ANOVA with Bonferroni post hoc test). The average of X biological replicates ± standard deviation is shown.

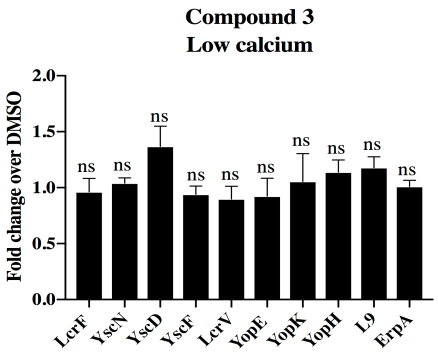
Compound 3
Low calcium
Fold change over DMSO
2.0
1.5
1.0
0.5
0.0
ns
ns
ns
ns
ns
ns
ns
ns
ns
ns
LcrF
YscN
YscD
YscF
LcrV
YopE
YopK
YopH
L9
ErpA

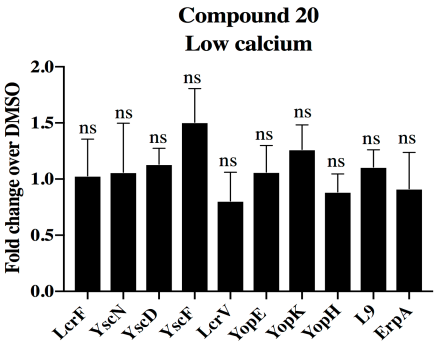
Compound 20
Low calcium
Fold change over DMSO
2.0
1.5
1.0
0.5
0.0
ns
ns
ns
ns
ns
ns
ns
ns
ns
ns
LcrF
YscN
YscD
YscF
LcrV
YopE
YopK
YopH
L9
ErpA

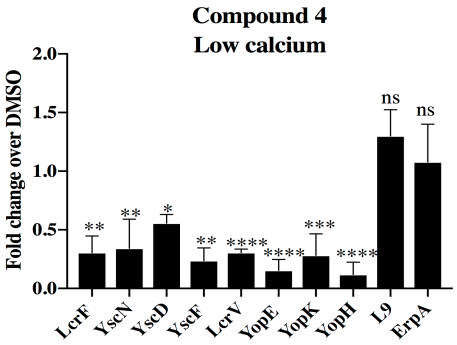
Compound 4
Low calcium
Fold change over DMSO
2.0
1.5
1.0
0.5
0.0
**
**
*
**
****
****
***
****
ns
ns
LcrF
YscN
YscD
YscF
LcrV
YopE
YopK
YopH
L9
ErpA

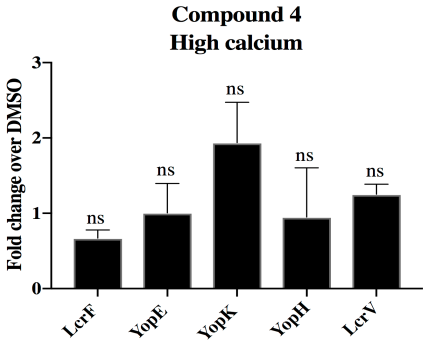
Compound 4
High calcium
Fold change over DMSO
3
2
1
0
ns
ns
ns
ns
ns
LcrF
YopE
YopK
YopH
LcrV

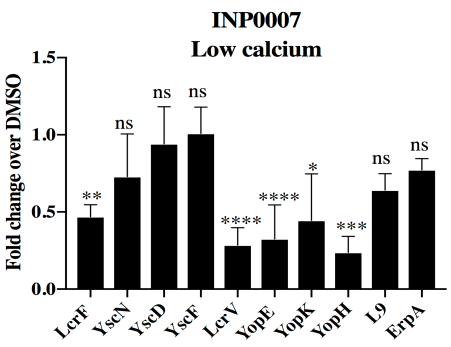
INP0007
Low calcium
Fold change over DMSO
1.5
1.0
0.5
0.0
**
ns
ns
ns
****
****
*
***
ns
ns
LcrF
YscN
YscD
YscF
LcrV
YopE
YopK
YopH
L9
ErpA

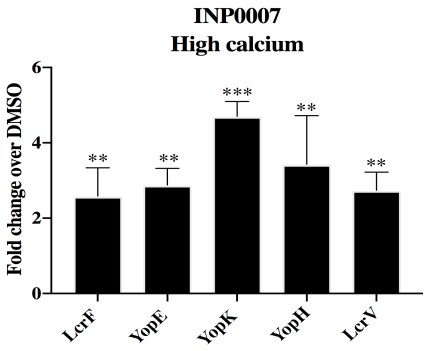
INP0007
High calcium
Fold change over DMSO
6
4
2
0
**
**
***
**
**
LcrF
YopE
YopK
YopH
LcrV

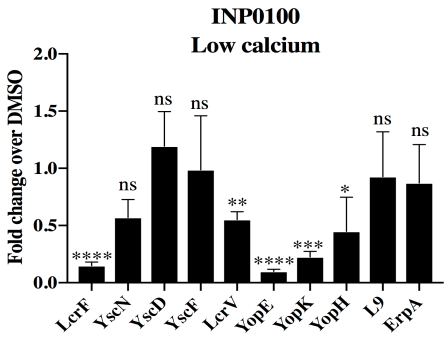
INP0100
Low calcium
Fold change over DMSO
2.0
1.5
1.0
0.5
0.0
****
ns
ns
ns
**
****
***
*
ns
ns
LcrF
YscN
YscD
YscF
LcrV
YopE
YopK
YopH
L9
ErpA

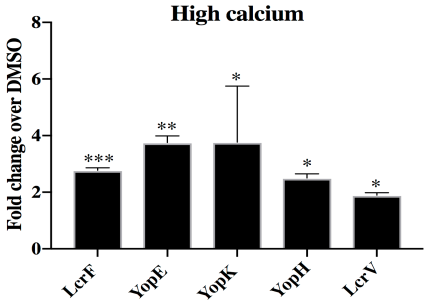
INP0010
High calcium
Fold change over DMSO
8
6
4
2
0
***
**
*
*
*
LcrF
YopE
YopK
YopH
LcrV

Figure 4. T3SS gene mRNA levels under low and high calcium conditions. Wildtype *Y. pseudotuberculosis* was grown under high or low calcium conditions in the presence of 50 μM compound or equivalent volume of DMSO and mRNA levels of T3SS (*lcrF*, *yscN*, *yscD*, *yscF*, *lcrV*, *yopE*, *yopK*, *yopH*) and non-T3SS genes (L9, *erpA*) assessed by qPCR. The average of X biological replicates ± standard error of the mean is shown. ****P<0.0001, ***P<0.0008, **P<0.004 (one way ANOVA with Bonferroni post hoc test). ns, not significant.

Assessment of T3SS assembly

In order to monitor T3SS assembly, we used fluorescence microscopy to quantify YscD in *Y. enterocolitica* and YscF puncta formation in *Y. pseudotuberculosis* as a proxy for T3SS basal body and T3SS needle assembly, respectively, as previously described (Davis and Mecsas 2007; Diepold et al. 2010; Morgan et al. 2017). Only INP0007 significantly impacted YscD-EGFP puncta formation (Figure 5). Importantly, the level of diffuse fluorescence in INP0007-treated *Yersinia* was greater than that of 26˚C-grown *Yersinia* (Figure 5A, inset), indicating that while YscD is expressed, it is not assembled into basal bodies in the presence of INP0007. In contrast, while C3 and C20 had no significant effect on YscF puncta formation as measured with an anti-YscF antibody, C4, INP0007, and INP0010 significantly inhibited needle assembly (Figure 6).

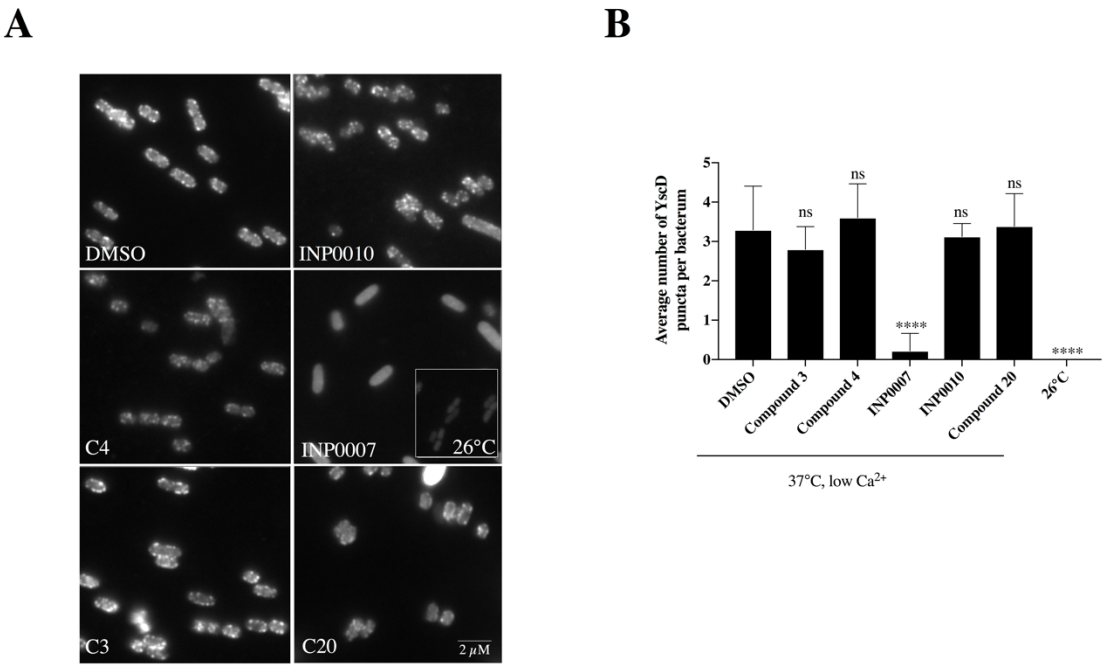

Figure 5. YscD-EGFP puncta formation in *Y. enterocolitica.*
Y. enterocolitica pYV40-EGFP-*yscD* was grown under T3SS-inducing conditions for three hours in the presence of 50 μM compound or equivalent volume of DMSO and fluorescent foci quantified using IMARIS software. Representative images **(A)** and the average number of foci ± standard deviation per cell **(B)** are shown from three biological replicates, with N>2000 cells quantified per condition. **** P<0.007 (one way ANOVA with Bonferroni post hoc).

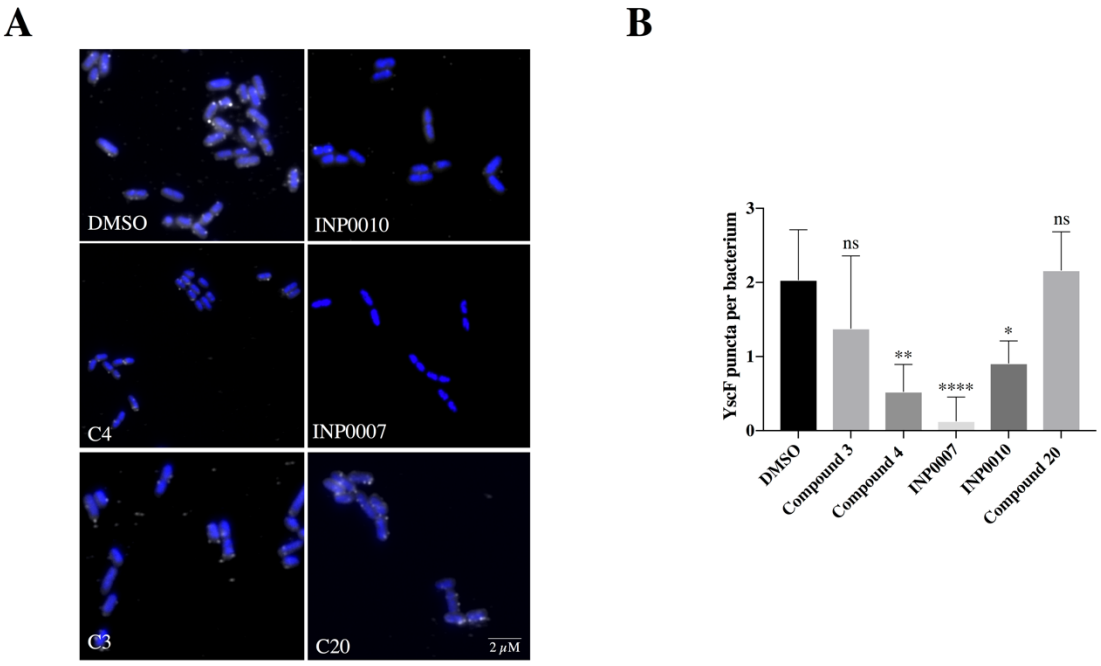

Figure 6. YscF puncta visualization in *Y. pseudotuberculosis* using immunofluorescence. Wildtype *Y. pseudotuberculosis* was grown under T3SS-inducing conditions for three hours in 50 μM compound or equivalent volume of DMSO and an anti-YscF antibody used to visualize T3SS needles. **(A)** Representative confocal microscopy images and **(B)** the average number of YscF puncta per bacterium from three biological replicates ± the standard deviation are shown, with N>1500 bacteria quantified per condition. *, P= 0.0377; ** P=0.0012; **** P<0.0001 (one way ANOVA with Bonferroni post hoc).

The bacterial flagellar apparatus is composed of a basal body that is structurally related to the injectisome T3SS basal body and mediates secretion of the flagellar hook and filament proteins (Macnab 2004). Therefore, it is possible that compounds with the ability to inhibit injectisome T3SS basal body assembly may inhibit flagellar assembly and therefore flagellar motility. INP0007 has been shown to inhibit motility in *Yersinia* (Kauppi et al. 2003), but neither INP0007 nor INP0010 inhibit motility in *Salmonella* (Negrea et al. 2007). In our standard *Yersinia* motility agar (Morgan et al.

2017), INP0007 significantly decreased flagellar motility in *Y. pseudotuberculosis*, while INP0010 did not (Figure 7). However, addition of the chelating agent EGTA in the motility agar, as used in the Kaupii et al study (Kauppi et al. 2003), led to both INP0007 and INP0010 having a significant inhibitory effect on motility (Figure 7).

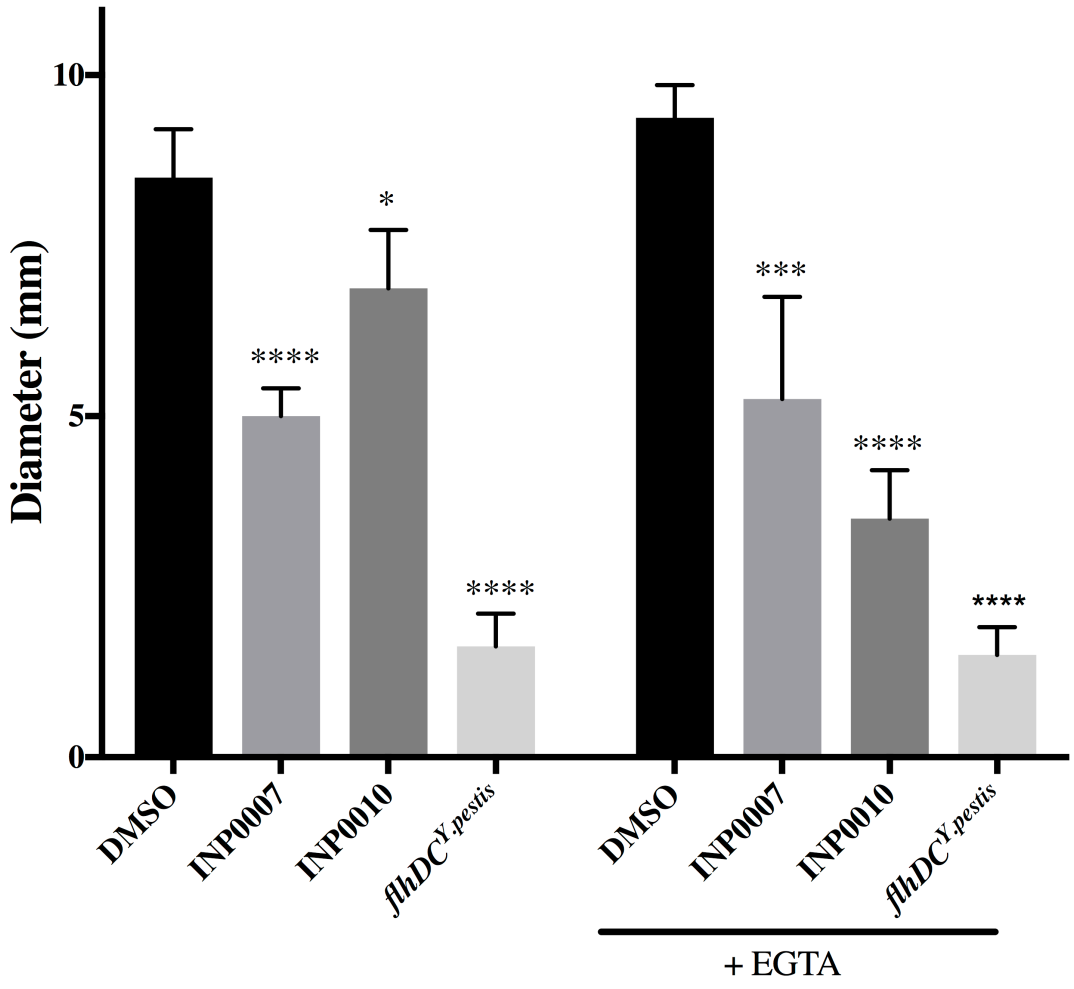

Figure 7. INP0007 and INP0010 inhibit *Y. pseudotuberculosis* motility. Y. pseudotuberculosis wildtype or the non-motile *flhDC*$^{Y.pestis}$ mutant were spotted onto motility agar containing the 50 µM compounds or the equivalent volume of DMSO and allowed to grow for ~30 hours. Average swimming diameter of the colony was

measured from three biological replicates ± standard deviation. **** P<0.0001, ***P=0.0002, *P=0.0217 (one way ANOVA with Bonferroni post hoc compared to DMSO in their respective condition)

Assessment of effector protein translocation

One of the most important requirements of a T3SS inhibitor is its ability to prevent translocation of effector proteins into target host cells. We employed a YopM-β-lactamase reporter assay to assess translocation of effector proteins into CHO K1 cells loaded with CCF2, a fluorescent β-lactamase substrate (Dewoody et al. 2011). While C3, C4, C20, INP0007 and INP0010 significantly blocked YopM-β-lactamase translocation at 50µM, however INP0010 appeared to be cytotoxic at this concentration (Figure 8).

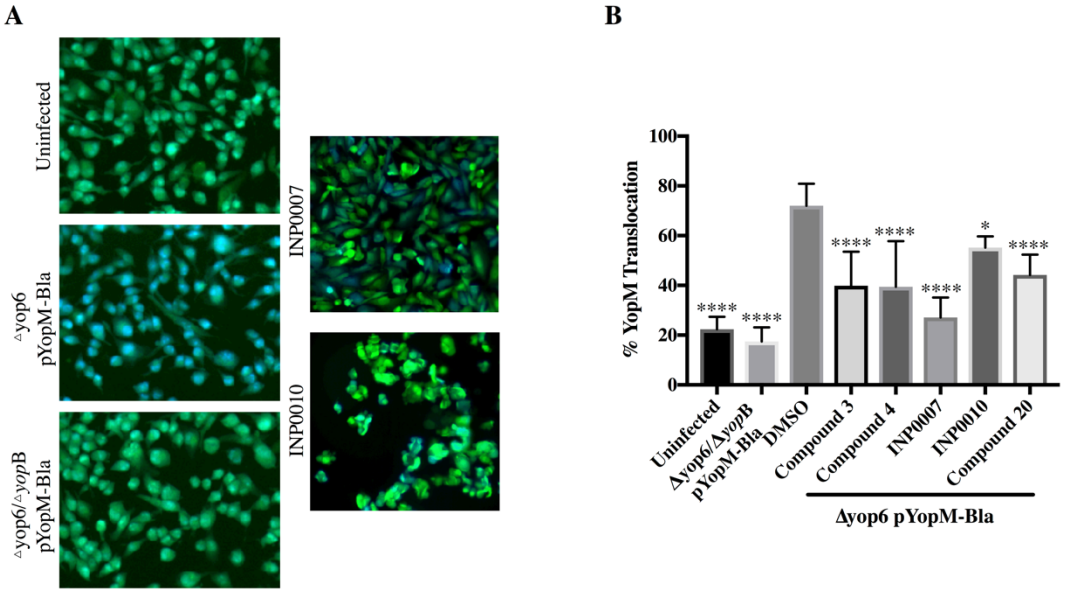

Figure 8. Translocation of YopM-Bla into mammalian cells in the presence of T3SS inhibitors. (A) Representative fluorescent micrographs of CCF2-AM loaded CHO K1 cells in the absence of bacterium (uninfected) or infected for two hours with *Y. pseudotuberculosis* lacking YopHEMOJT but expressing the Yop reporter YopM-

Bla (Δyop6 pYopM-Bla) at MOI 7 in the presence of 50 μM compound or equivalent volume of DMSO. A T3SS-defective mutant lacking the pore-forming protein YopB was used as a negative control (Δyop6/Δ*yopB* pYopM-Bla). **(B)** CCF2 green (uncleaved) and blue (cleaved) fluorescence was measured and the average from three biological replicates ± standard deviation is shown. *, P <0.05; ***, P< 0.001; ****P<0.0001 (one way ANOVA with Bonferroni post hoc test).

DISCUSSION

A methodical approach to primary characterization of inhibitors for the T3SS has been lacking in the field. Here we describe a pipeline of miniaturized assays, using enteropathogenic *Yersinia* as the workhorse organism, that enable rapid, initial characterization of the stage of T3SS expression, assembly, or function targeted by compounds with T3SS inhibitory activity. Furthermore, we used a training set of compounds with previously-identified T3SS inhibitory activity to test the utility of this pipeline.

One compound in our training set, C3, blocked the ability of the *Yersinia* T3SS both to secrete T3SS effector proteins into low calcium culture supernatant and to translocate effector proteins into target host cells. Yet C3 did not block T3SS basal body and needle assembly, as determined by imaging YscD basal body and YscF needle puncta formation. C3 showed a modest inhibition of YopE secretion (28%), but notably inhibited secretion of the translocator proteins, YopB and D. These data provide a possible explanation for why C3 strongly inhibited Yop translocation into host cells (40%) despite less potent inhibition of YopE secretion, as YopB and YopD are required for Yop delivery into host cells (Montagner et al. 2011). C3 has

structural similarities with the phenoxyacetamides, which target the SctF needle subunit (Aiello et al. 2010; Bowlin et al. 2014). However, our data indicate that C3 blocks a specific activity of the assembled T3SS. Alternatively, the T3SS needle structure may be altered in the presence of C3, still allowing recognition by our anti-YscF antibody but impeding cargo egress. Importantly, the results from our experiment pipeline significantly narrow down the possible modes of action of C3 and provide testable hypotheses.

In contrast to C3, C20 specifically blocked translocation of a T3SS effector protein into host cells without blocking any other stage of type III secretion, including T3SS effector protein secretion into low calcium culture. As C20 was previously shown to inhibit only translocation of T3SS effector proteins into target host cells (Harmon et al. 2010), our verification of this finding further demonstrates the robustness of our experimental pipeline. Harmon et al. hypothesized that C20 inhibited the host cell-bacterial interaction, as C20 strongly inhibited adherence of *Y. pseudotuberculosis* to HEp-2 cells. Possible modes of action of compounds that inhibit Yop translocation but not any other stage of type III secretion include interruption of bacterial adhesins, host integrin receptors, or YopBD-mediated pore formation on the host membrane.

While none of the inhibitors we tested affected pYV copy number, our data shows that prevention of T3SS plasmid copy number upregulation during active type III secretion leads to dramatically reduced T3SS gene mRNA steady-state levels.

Therefore, when using *Yersinia* as a model organism for assessing T3SS inhibitor mechanism of action, it is important to consider pYV copy number. Furthermore, as chloramphenicol and rifampicin significantly inhibited luminescence as a readout of pYV copy number, this assay also sheds light on whether a compound affects general transcription or translocation. One caveat is that compounds that act as luminescence quenchers would decrease luminescence in this assay. In this case, analyzing expression of non-T3SS genes, such as the L9 and ErpA genes shown here, via qPCR can serve as a way to test this possibility.

C4 was shown to inhibit promoter activity of *lcrF*, the Ysc T3SS master regulator (Kauppi et al. 2003). However, while we observed a C4-dependent decrease in mRNA levels of all T3SS genes tested under low calcium T3SS-inducing conditions, C4 treatment did not impact T3SS gene expression under high calcium conditions when T3SSs are assembled but no Yop secretion occurs. As a Δ*lcrF* mutant had significantly less T3SS gene expression under high calcium conditions compared to wildtype *Yersinia*, this argues against C4 inhibiting LcrF activity. C4 did not alter the number of YscD puncta observed but did decrease the number of YscF puncta per cell by greater than half. These data suggest that C4 does not impact YscD assembly in the plasma membrane but disrupts overall T3SS basal body formation in such a way that needle formation is compromised or interferes with YscF secretion or assembly.

The salicylidene acylhydrazides INP0007 and INP0010 inhibited expression of *lcrF*, *lcrV*, and *yopKEH*, but did not decrease expression of *yscN*, *yscD* or *yscF*. While INP0007 and INP0010 are related structurally, INP0010 prevents *Yersinia* growth if the bacteria are exposed longer than six hours, while INP0007 does not affect bacterial growth even up to 13 hours of exposure. Surprisingly, while INP0010 did not inhibit YscD puncta formation, INP0007 caused a 10-fold decrease in YscD puncta. Both compounds significantly inhibited YscF puncta formation, Yop secretion into low calcium culture, and Yop translocation into host cells. However, measuring Yop translocation into host cells in the presence of INP0010 is complicated by the obvious toxic effects of the compound on host cells. Therefore, utilization of the Yop translocation assay of our experimental pipeline is limited to compounds without toxic effects on host cells. However, this also shows the benefit of using microscopy to observe CCF2 green-to-blue fluorescence conversion, as it allows observation of host cell morphology. The salicylidene acylhydrazide class of compounds have been suggested to have a broad impact on expression of horizontally acquired genes (Tree et al. 2009). However, we only observe a defect in T3SS gene expression in low calcium, but not high calcium medium, for INP0007. In addition, we observe a significant defect in flagellar motility by INP0007, suggesting a broader effect of the compound either on the flagellar T3SS, ATP synthesis, or the proton motive force. In total, our results argue that INP0007 inhibits formation of the injectisome T3SS and, either through a similar mechanism or by targeting multiple pathways, also disrupts flagellar T3SS activity.

Given the previously-demonstrated positive feedback exerted by active type III secretion on T3SS gene transcription (Cornelis et al. 1987), we expected that C3 would inhibit T3SS gene expression in low calcium medium. C4, INP0007, and INP0010 inhibited secretion by 90-100% and this correlated with the ability to affect T3SS gene expression under low calcium conditions. C3 only inhibited secretion less than 28% and this was insufficient to affect the feedback loop on T3SS gene expression. Furthermore, the T3SS inhibitor piericidin A1 inhibits Yop secretion by ~40-45% and also does not repress transcription of T3SS genes (Morgan et al. 2017). These data suggest that only compounds that almost completely inhibit Yop secretion will affect the T3SS gene expression feedback loop. This suggests that screening strategies based on Yop gene expression as the readout for T3SS inhibition may miss less robust compounds that could be improved by structure-activity relationship analysis.

In summary, the experimental pipeline described here can be used to rapidly bin T3SS inhibitors into categories depending on the stage of type III secretion they inhibit. In addition, validation of this pipeline with a training set of previously-identified T3SS inhibitors provided testable hypotheses to explore modes of action.

ACKNOWLEDGEMENTS

We thank Benjamin Abrams of the UCSC Life Sciences Microscopy Center and

Walter Bray of the UCSC Chemical Screening Center for technical support. We thank Andreas Diepold for providing the fluorescent YscD *Y. enterocolitica* strain.

Author contribution statement

JM- experimental design, performing experiments, writing paper

JD – performing experiments

JL – performing experiments

HL- experimental design

SM, RI, HW- providing reagents

VA- experimental design, writing paper

Conflict of Interest Statement

The authors have no conflict of interest to disclose.

REFERENCES

Aiello D, Williams JD, Majgier-Baranowska H, Patel I, Peet NP, Huang J, Lory S, Bowlin TL, Moir DT. 2010. Discovery and characterization of inhibitors of pseudomonas aeruginosa type iii secretion. Antimicrob Agents Chemother. 54(5):1988-1999.

Anantharajah A, Buyck JM, Sundin C, Tulkens PM, Mingeot-Leclercq MP, Van Bambeke F. 2017. Salicylidene acylhydrazides and hydroxyquinolines act as

inhibitors of type three secretion systems in pseudomonas aeruginosa by distinct mechanisms. Antimicrob Agents Chemother. 61(6).

Andersen JB, Sternberg C, Poulsen LK, Bjorn SP, Givskov M, Molin S. 1998. New unstable variants of green fluorescent protein for studies of transient gene expression in bacteria. Appl Environ Microbiol. 64(6):2240-2246.

Auerbuch V, Golenbock DT, Isberg RR. 2009. Innate immune recognition of yersinia pseudotuberculosis type iii secretion. PLoS Pathog. 5(12):e1000686.

Beckham KS, Roe AJ. 2014. From screen to target: Insights and approaches for the development of anti-virulence compounds. Front Cell Infect Microbiol. 4:139.

Bergeron J, Worrall L, Sgourakis N, DiMaio F, Pfuetzner R, Felise H, Vuckovic M, Yu A, Miller S, Baker D et al. 2013. A refined model of the prototypical salmonella spi-1 t3ss basal body reveals the molecular basis for its assembly. Plos Pathogens. 9(4).

Berube BJ, Murphy KR, Torhan MC, Bowlin NO, Williams JD, Bowlin TL, Moir DT, Hauser AR. 2017. Impact of type iii secretion effectors and of phenoxyacetamide inhibitors of type iii secretion on abscess formation in a mouse model of pseudomonas aeruginosa infection. Antimicrob Agents Chemother. 61(11).

Bowlin NO, Williams JD, Knoten CA, Torhan MC, Tashjian TF, Li B, Aiello D, Mecsas J, Hauser AR, Peet NP et al. 2014. Mutations in the pseudomonas aeruginosa needle protein gene pscf confer resistance to phenoxyacetamide

inhibitors of the type iii secretion system. Antimicrob Agents Chemother. 58(4):2211-2220.

Broz P, Mueller CA, Müller SA, Philippsen A, Sorg I, Engel A, Cornelis GR. 2007. Function and molecular architecture of the yersinia injectisome tip complex. Mol Microbiol. 65(5):1311-1320.

Büttner D, Bonas U. 2002. Port of entry--the type iii secretion translocon. Trends Microbiol. 10(4):186-192.

Coburn B, Sekirov I, Finlay B. 2007. Type iii secretion systems and disease. Clinical Microbiology Reviews. 20(4):535-+.

Cornelis G, Vanootegem JC, Sluiters C. 1987. Transcription of the yop regulon from y. Enterocolitica requires trans acting pyv and chromosomal genes. Microb Pathog. 2(5):367-379.

Davis A, Mecsas J. 2007. Mutations in the yersinia pseudotuberculosis type iii secretion system needle protein, yscf, that specifically abrogate effector translocation into host cells. Journal of Bacteriology. 189(1):83-97.

Deng W, Marshall NC, Rowland JL, McCoy JM, Worrall LJ, Santos AS, Strynadka NCJ, Finlay BB. 2017. Assembly, structure, function and regulation of type iii secretion systems. Nat Rev Microbiol. 15(6):323-337.

Dewoody R, Merritt PM, Houppert AS, Marketon MM. 2011. Yopk regulates the yersinia pestis type iii secretion system from within host cells. Mol Microbiol. 79(6):1445-1461.

Diepold A, Amstutz M, Abel S, Sorg I, Jenal U, Cornelis GR. 2010. Deciphering the assembly of the yersinia type iii secretion injectisome. The EMBO journal. 29(11):1928-1940.

Duncan MC, Linington RG, Auerbuch V. 2012. Chemical inhibitors of the type three secretion system: Disarming bacterial pathogens. Antimicrob Agents Chemother. 56(11):5433-5441.

Fahlgren A, Avican K, Westermark L, Nordfelth R, Fällman M. 2014. Colonization of cecum is important for development of persistent infection by yersinia pseudotuberculosis. Infect Immun. 82(8):3471-3482.

Forsberg A, Wolf-Watz H. 1988. The virulence protein yop5 of yersinia pseudotuberculosis is regulated at transcriptional level by plasmid-plb1 -encoded trans-acting elements controlled by temperature and calcium. Mol Microbiol. 2(1):121-133.

Francis MS, Wolf-Watz H, Forsberg A. 2002. Regulation of type iii secretion systems. Curr Opin Microbiol. 5(2):166-172.

Harmon DE, Davis AJ, Castillo C, Mecsas J. 2010. Identification and characterization of small-molecule inhibitors of yop translocation in yersinia pseudotuberculosis. Antimicrob Agents Chemother. 54(8):3241-3254.

Heroven AK, Böhme K, Dersch P. 2012. The csr/rsm system of yersinia and related pathogens: A post-transcriptional strategy for managing virulence. RNA Biol. 9(4):379-391.

Horton RM, Cai ZL, Ho SN, Pease LR. 1990. Gene splicing by overlap extension: Tailor-made genes using the polymerase chain reaction. Biotechniques. 8(5):528-535.

Karzai AW, Roche ED, Sauer RT. 2000. The ssra-smpb system for protein tagging, directed degradation and ribosome rescue. Nat Struct Biol. 7(6):449-455.

Kauppi AM, Nordfelth R, Uvell H, Wolf-Watz H, Elofsson M. 2003. Targeting bacterial virulence: Inhibitors of type iii secretion in yersinia. Chem Biol. 10(3):241-249.

Macnab RM. 2004. Type iii flagellar protein export and flagellar assembly. Biochim Biophys Acta. 1694(1-3):207-217.

Marsden AE, Intile PJ, Schulmeyer KH, Simmons-Patterson ER, Urbanowski ML, Wolfgang MC, Yahr TL. 2016. Vfr directly activates exsa transcription to regulate expression of the pseudomonas aeruginosa type iii secretion system. J Bacteriol. 198(9):1442-1450.

Marshall NC, Finlay BB. 2014. Targeting the type iii secretion system to treat bacterial infections. Expert Opin Ther Targets. 18(2):137-152.

Mehigh RJ, Sample AK, Brubaker RR. 1989. Expression of the low calcium response in yersinia pestis. Microb Pathog. 6(3):203-217.

Miller HK, Kwuan L, Schwiesow L, Bernick DL, Mettert E, Ramirez HA, Ragle JM, Chan PP, Kiley PJ, Lowe TM et al. 2014. Iscr is essential for yersinia pseudotuberculosis type iii secretion and virulence. PLoS Pathog. 10(6):e1004194.

Montagner C, Arquint C, Cornelis GR. 2011. Translocators yopb and yopd from yersinia enterocolitica form a multimeric integral membrane complex in eukaryotic cell membranes. J Bacteriol. 193(24):6923-6928.

Morgan JM, Duncan MC, Johnson KS, Diepold A, Lam H, Dupzyk AJ, Martin LR, Wong WR, Armitage JP, Linington RG et al. 2017. Piericidin a1 blocks yersinia ysc type iii secretion system needle assembly. mSphere. 2(1).

Negrea A, Bjur E, Ygberg SE, Elofsson M, Wolf-Watz H, Rhen M. 2007. Salicylidene acylhydrazides that affect type iii protein secretion in salmonella enterica serovar typhimurium. Antimicrob Agents Chemother. 51(8):2867-2876.

Nordfelth R, Kauppi AM, Norberg HA, Wolf-Watz H, Elofsson M. 2005. Small-molecule inhibitors specifically targeting type iii secretion. Infect Immun. 73(5):3104-3114.

Perry RD, Harmon PA, Bowmer WS, Straley SC. 1986. A low-ca2+ response operon encodes the v antigen of yersinia pestis. Infect Immun. 54(2):428-434.

Pettersson J, Nordfelth R, Dubinina E, Bergman T, Gustafsson M, Magnusson KE, Wolf-Watz H. 1996. Modulation of virulence factor expression by pathogen target cell contact. Science. 273(5279):1231-1233.

Portnoy DA, Moseley SL, Falkow S. 1981. Characterization of plasmids and plasmid-associated determinants of yersinia enterocolitica pathogenesis. Infect Immun. 31(2):775-782.

Sample AK, Fowler JM, Brubaker RR. 1987. Modulation of the low-calcium response in yersinia pestis via plasmid-plasmid interaction. Microb Pathog. 2(6):443-453.

Schwiesow L, Lam H, Dersch P, Auerbuch V. 2015. Yersinia type iii secretion system master regulator lcrf. J Bacteriol. 198(4):604-614.

Skinner SO, Sepúlveda LA, Xu H, Golding I. 2013. Measuring mrna copy number in individual escherichia coli cells using single-molecule fluorescent in situ hybridization. Nat Protoc. 8(6):1100-1113.

Straley SC, Bowmer WS. 1986. Virulence genes regulated at the transcriptional level by ca2+ in yersinia pestis include structural genes for outer membrane proteins. Infect Immun. 51(2):445-454.

Tree JJ, Wang D, McInally C, Mahajan A, Layton A, Houghton I, Elofsson M, Stevens MP, Gally DL, Roe AJ. 2009. Characterization of the effects of salicylidene acylhydrazide compounds on type iii secretion in escherichia coli o157:H7. Infect Immun. 77(10):4209-4220.

Veenendaal AK, Sundin C, Blocker AJ. 2009. Small-molecule type iii secretion system inhibitors block assembly of the shigella type iii secreton. J Bacteriol. 191(2):563-570.

Wang H, Avican K, Fahlgren A, Erttmann SF, Nuss AM, Dersch P, Fallman M, Edgren T, Wolf-Watz H. 2016. Increased plasmid copy number is essential for yersinia t3ss function and virulence. Science. 353(6298):492-495.

Wilharm G, Lehmann V, Krauss K, Lehnert B, Richter S, Ruckdeschel K, Heesemann J, Trülzsch K. 2004. Yersinia enterocolitica type iii secretion depends on the proton motive force but not on the flagellar motor components mota and motb. Infection and Immunity.

Yother J, Goguen JD. 1985. Isolation and characterization of ca2+-blind mutants of yersinia pestis. J Bacteriol. 164(2):704-711.

CHAPTER 3

Piericidin A1 Blocks Yersinia Ysc Type III Secretion System Needle Assembly

By: Jessica M. Morgan, Miles C. Duncan, Kevin S. Johnson, Andreas Diepold, Hanh Lam, Allison J. Dupzyk, Lexi R. Martin, Weh Ruh Wong, Judith P. Armitage, Roger G. Linington, Victoria Auerbuch

ABSTRACT

The type III secretion system (T3SS) is a bacterial virulence factor expressed by dozens of Gram-negative pathogens, but is largely absent from commensals. The T3SS is an attractive target for antimicrobial agents that may disarm pathogenic bacteria while leaving commensal populations intact. We previously identified piericidin A1 as an inhibitor of the Ysc T3SS in *Yersinia pseudotuberculosis.* Piericidins were first discovered as inhibitors of complex I of the electron transport chain in mitochondria and some bacteria. However, we found that piericidin A1 did not alter *Yersinia* membrane potential nor inhibit flagellar motility powered by the proton motive force, indicating that the piericidin mode of action against *Yersinia* type III secretion is independent of complex I. Instead, piericidin A1 reduced the number of T3SS needle complexes visible by fluorescence microscopy at the bacterial surface, preventing T3SS translocator and effector protein secretion. Furthermore, piericidin A1 decreased the abundance of higher order YscF needle subunit complexes, suggesting that piericidin A1 blocks YscF needle assembly. While expression of T3SS components in *Yersinia* are positively regulated by active type III secretion, the block in secretion by piericidin A1 was not accompanied by a decrease in T3SS gene expression, indicating that piericidin A1 may target a T3SS regulatory circuit. However, piericidin A1 still inhibited effector protein secretion in the absence of the T3SS regulators YopK, YopD, or YopN. Surprisingly, while piericidin A1 also inhibited the *Y. enterocolitica* Ysc T3SS, it did not inhibit the SPI-1 family Ysa T3SS in *Y. enterocolitica* nor the Ysc family T3SS in *Pseudomonas*

aeruginosa. Together, these data indicate that piericidin A1 specifically inhibits *Yersinia* Ysc T3SS needle assembly.

INTRODUCTION

Piericidins are a family of natural products produced by Actinobacteria that resemble coenzyme Q, also known as ubiquinone, a molecule heavily involved in electron transport in prokaryotes and eukaryotes alike (1). The piericidin family member piericidin A1 was originally shown to be a potent inhibitor of NADH oxidase in purified beef heart mitochondria (2). Subsequently, analysis of piericidin A1 resistant mutants in the bacterium *Rhodobacter capsalatus* suggested the molecular target to be the 49 kDa subunit of NADH-ubiquinone oxidoreductase, referred to as complex I (3). Complex I is large protein complex, containing at least 40 subunits with a mass of ~1 MDa, that is a central component of the electron transport chain in eukaryotes and prokaryotes (4). This complex functions to translocate protons and is integral in generating a proton gradient for ATP synthesis and other processes such as powering protein secretion. Piericidin A1 acts through blocking reduction of coenzyme Q by complex I (3, 5). Many bacteria are insensitive to piericidin, likely due to differences in complex I subunit composition and/or substrate and cofactor binding interfaces (6), possibly preventing piericidins from binding. Piericidin A1 has been explored as a potential anticancer agent, as treatment with nanomolar concentrations of the compound prevented upregulation of the glucose receptor GRP78, resulting in rapid cell death in glucose starved HT-29 cells (7), a human cultured colon cancer cell line. More recently, Kang et al. described

piericidin A1 as an inhibitor of quorum sensing in *Erwinia carotovora*, a potato plant pathogen, although the mechanism underlying this remains unclear (8).

Recently, we identified piericidin A1 and the piericidin derivative Mer-A 2026B as inhibitors of the bacterial type III secretion system (T3SS) (9). The T3SS is a complex nanomachine comprised of more than 20 different structural proteins, which assemble into a needle like injection apparatus that punctures eukaryotic cells and acts as a conduit through which bacterial effector proteins enter the host cell cytosol (10). Protein secretion through this apparatus requires a proton motive force (11) as well as the ATPase YscN (12), and is assembled in three stages. The basal body, assembled first, is composed of rings that embed in the inner and outer membrane of the bacterium and bridge the gap of the periplasmic space. Upon completion of the basal body, secretion of the 'early' T3SS substrates begins. The SctF needle subunit, referred to as YscF in *Yersinia*, is secreted at this stage and polymerizes from the basal body to form a hollow needle protruding ~60 nm into the extracellular space (13). Upon completion of needle assembly, a substrate specificity switch leads to secretion of the 'middle' substrates which comprise the pore or translocon complex (10). These three additional proteins, in *Yersinia* called YopD, YopB, and LcrV, are secreted and form the translocon complex at the tip of the newly polymerized YscF needle (14). YopK (YopQ in *Yersinia enterocolitica*) has been shown to regulate translocation of the pore-forming translocon proteins YopB and YopD as well as effector Yops (15). In addition to its role as a translocon protein, YopD is thought to form a complex with LcrQ and LcrH to bind Yop mRNA and the

30s ribosomal subunit, inhibiting translation until the T3SS is actively secreting cargo including LcrQ and YopD (16, 17). The final substrate switch, to the secretion of 'late' cargo, T3SS effector proteins called Yops in *Yersinia* and regulatory proteins, is triggered *in vivo* by host cell contact, which may be sensed by the translocon (18). In *Yersinia*, this response can be mimicked through the chelation of calcium (19, 20). Therefore, secretion of late Yops is prevented in the presence of high calcium, and permitted under low calcium. In *Yersinia*, the regulatory proteins YopN and TyeA prevent secretion of Yops prior to host cell contact or a decrease in calcium concentration (21, 22).

We previously identified piericidin A1 as an inhibitor of the T3SS in *Yersinia pseudotuberculosis.* In this study, we characterize the activity of piericidin A1 on the type III secretion systems of the related gut pathogens *Yersinia pseudotuberculosis* and *Y. enterocolitica*, as well as the opportunistic pathogen *Pseudomonas aeruginosa*.

MATERIALS AND METHODS

Bacterial Strains and Growth Conditions. Bacterial strains used in this paper are listed in Table 1. *Y. pseudotuberculosis* was grown in 2xYT (yeast extract-tryptone) at 26°C with shaking overnight. The cultures were back-diluted into low calcium media (2xYT plus 20 mM sodium oxalate and 20 mM $MgCl_2$) to an optical density (OD_{600}) of 0.2 and grown for 1.5 hours at 26°C shaking followed by 1.5 hours at 37˚C to induce Yop synthesis as previously described (23). *Pseudomonas aeruginosa* was grown in Luria-Bertani broth at 37°C with shaking. *Y. enterocolitica* was grown in 1%

tryptone/0.5% yeast extract at 26˚C shaking overnight.

The full length *yopD* deletion mutation (24), leaving only the first three and last three amino acids of YopD, was constructed using the primers described in (25). The *yopK* deletion mutation was introduced into *Y. pseudotuberculosis* using a pSR47s-derived suicide plasmid obtained from Molly Bergman (24). *Y. pseudotuberculosis* Δ*yopD* and Δ*yopK* mutants were isolated as previously described (24).

Strain	Mutation	Reference
Yersinia pseudotuberculosis		
Wildtype	IP2666pIB1	(53)
Δ*yscNU*	Δ*yscNU*	(52)
Δ*yopN*	Δ*yopN*	(43)
Δ*yopK*	Δ*yopK*	This study
Δ*yopD*	Δ*yopD*	This study
***flhDC*$^{Y.pestis}$**	Δ*yopHEMOJ*/*flhDC*$^{Y.pestis}$	(23)
pYscF	Δ*yopHEMOJ*/*YscF*+ pTCR99-YscF	(30)
pEmpty	Δ*yopHEMOJ*/*YscF*+ pTCR99 empty vector	(30)
Pseudomonas aeruginosa		
Wildtype (PA103)	Expresses ExoU and ExoT effectors	(54, 55)
Yersinia enterocolitica		
yscL	*yscL*::mini-Tn5 *KM2*	(56)
ysaT	ysaT::Tn*Mod*-RKm’	(57)

Table 1. Bacterial strains used in this study.

Piericidin A1. Piericidin A1 was isolated from *Actinomycetes* strain RL09-253-HVS-A, isolated from a marine sediment sample collected by SCUBA at Point Estero, CA, at a depth of 50 feet. This *Actinomycetes* strain was identified as a *Streptomyces* sp. based on the typical morphology of streptomycetes, which form dry powdery spores on agar plates, and by sequencing the 16S rRNA gene (data not shown). From a large-scale culture (4 liters) of the strain in SYP medium was obtained an organic extract, which was subject to a stepwise eluotropic gradient on a 10 g C_{18} Sep Pak

cartridge (MeOH-H_2O gradient: 40 ml of 10%, 20% (fraction A), 40% (fraction B), 60% (fraction C), 80% (fraction D), and 100% (fraction E) MeOH and then 100% ethyl acetate (EtOAc) (fraction F)). 0.33 g of fraction D was obtained, and the active constituent purified using C_{18} RP-HPLC (gradient profile 58% to 88% MeOH/0.02% formic acid-H_2O; 2 ml/ min; Synergi 10 Fusion-RP column; Phenomenex, USA; t_R = 30.5 min) to give 2.7 mg of piericidin A1. Electrospray ionization-time of flight high-resolution mass spectrometry (ESI-TOF HRMS) analysis confirmed the molecular formula $C_{25}H_{37}NO_4$. This structure was confirmed by one-dimensional ^1H nuclear magnetic resonance (NMR) spectroscopy on a Varian Unity Inova spectrometer at 600 MHz and comparison with literature values. Piericidin A1 is commercially available, however mass spectroscopy on commercially available piericidin A1 found it to be impure (data not shown). We have observed that these impurities can lead to inconsistent and artefactual results (data not shown). The concentration of piericidin A1 used in our experiments, 71uM, is approximately twice the IC_{50} for Yop translocation (9).

Anti-YscF antibody. The anti-YscF antibody used in this study was raised in rabbits against the *Y. pseudotuberculosis* YscF peptide KDKPDNPALLADLQH (Pacific Immunology).

Measurement of Membrane Potential. Bacteria were grown under the type III secretion inducing conditions described above and membrane potential measured as previously described (26). Briefly, during the last 30 minutes of the 37°C incubation, JC-1, a fluorescent dye widely used to measure membrane potential, was added. As a

control, the protonophore, CCCP, was used. Samples were imaged using a LSM 5 PASCAL laser scanning microscope (Zeiss) fitted with a Plan-Apochromat 63x/1.4 Oil DIC objective and analyzed using the LSM 510 software (Zeiss). Quantification of image intensities was performed using ImageJ.

Type III secretion assay. Visualization of *Y. pseudotuberculosis* T3SS cargo secreted in broth culture was performed as previously described (23). *Y. pseudotuberculosis* low calcium media cultures were grown for 1.5 hrs at 26°C. Compounds or DMSO were added and the cultures were switched to 37°C for another 2 hrs. Coenzyme Q (Sigma) was resuspended in warm DMSO. For the type III secretion reversibility assay, following the 2 hr 37°C step, cultures were washed and incubated with piericidin A1 (71 uM) or the equivalent volume of DMSO for another 45 min before secreted proteins were isolated (27). To test dependence on protein synthesis, following the 2 hr 37°C step, cultures were washed and incubated with 5 μM chloramphenicol or an equal volume of 100% ethanol for another 45 minutes before secreted proteins were isolated or cells were fixed for microscopy experiments. To test the effect of CCCP, a compound that causes the uncoupling of the proton gradient, on secretion, overnight cultures were diluted 1:40 in BHI and grown 2 hours at 37°C. CCCP was then added at 10 μM and the culture allowed to shake for 5 minutes. Secretion was then induced by the addition of 5 mM EGTA and 10 mM $MgCl_2$. Cultures were collected at 5, 30, and 60 minutes after T3SS induction.

For *Pseudomonas aeruginosa*, overnight cultures were washed and resuspended in LB supplemented with 5 mM EGTA and 20 mM $MgCl_2$ with piericidin A1 (71 μM)

or DMSO and grown at 37°C for 3 hours (28). For *Y. enterocolitica* Ysa secretion, overnight cultures were grown in 1% tryptone/0.5% yeast extract (no salt L media) at 26˚C shaking overnight. The cultures were back-diluted into either no salt L media or with 290 mM NaCl added and incubated for 6 hours at 26˚C shaking, as previously described (29). Cultures were spun down at 13,200 rpm for 10 min at room temperature. Supernatants were transferred to a new eppendorf tube. For *Y. enterocolitica* supernatants, the upper two-thirds only were removed and centrifuged again. The upper two-thirds were removed once again and passed through a 0.22 μm filter prior to TCA precipitation. Ten percent final trichloroacetic acid (TCA) was added and the mixture vortexed vigorously. Samples were incubated on ice for 20 min and then spun down at 13,200 rpm for 15 min at 4°C. The pellet was resuspended in final sample buffer (FSB) + 20% DTT. Samples were boiled for 15 min prior to running on a 12.5% SDS-PAGE gel. Sample loading was normalized for bacterial density (OD_{600}) of each sample. *Y. pseudotuberculosis* and *P. aeruginosa* samples were visualized with coomassie blue staining while *Y. enterocolitica* Ysa samples were visualized with SYPRO® Ruby (Molecular Probes). Densitometric quantification of the bands was done using Image Lab software (Bio-Rad), setting the relevant DMSO-treated *Y. pseudotuberculosis* YopE band to 1.00.

Secreted and Cytosolic YopE Western Blot. Supernatant samples were obtained as described above in the type III secretion assay. In parallel, after the supernatant was collected, the pellet was resuspended in the same volume of final sample buffer (FSB) + 20% DTT as the corresponding supernatant sample. The pellet samples were then

boiled for 15 min. Cytosolic and secreted protein samples were run on a 12.5% SDS-PAGE gel and transferred to a blotting membrane (Immobilon-P) by a Trans-Blot semi-dry transfer cell (BioRad). Blots were blocked overnight in TBST with 5% skim milk, and probed with YopE primary antibody and horseradish peroxidase secondary (Santa Cruz Biotech). Following visualization, densitometric quantification of the bands was performed using Image Lab software (Bio-Rad), setting the first DMSO-treated WT *Y. pseudotuberculosis* YopE band to 1.00.

Detection of Secreted Monomeric YscF. As we could not detect secreted monomeric YscF from wildtype bacteria, presumably because it becomes rapidly polymerized into the needle structure, we used a strain of *Y. pseudotuberculosis* that ectopically expresses YscF from an IPTG inducible pTCR99A plasmid (pYscF). Cultures were grown overnight in 2xYT with 100 ug/mL carbenicillin. The following day, cultures were back diluted to OD_{600} 0.2 in low calcium medium plus carbenicillin and were grown at 26°C for 1.5 hours. At the 37°C shift, 10 μM IPTG and either 71 μM piericidin A1 or DMSO were added to cultures and allowed to incubate 2 hours. After incubation bacteria were normalized by OD_{600} and a TCA was preformed as described above.

Crosslinking Assay. *Yersinia* carrying YscF on an IPTG inducible plasmid (pYscF) was grown under the T3SS inducing conditions described above. At the 37°C shift, 10 μM IPTG was added to induce YscF expression. After a 2 hour induction the cells were collected and the crosslinker BS^3 was added as previously described (30). Samples were boiled in Laemelli buffer and pulled through a 25 gauge needle several

times to shear genomic DNA. Samples were loaded onto a 16.5% Tris-Tricine gel (Bio-Rad) and run at 120V. Proteins were transferred to a PVDF membrane (Immobilon-P) using mini transblot cell (Biorad), and probed with YscF antibody (1:10,000) overnight followed by horseradish peroxidase secondary (Santa Cruz Biotech).

Motility Assay. Following overnight growth, bacterial cultures were diluted to an optical density of 2.5. One µl of WT *Y. pseudotuberculosis* or a non-motile mutant expressing $flhDC^{Y.\ pestis}$ (23) were spotted onto motility media (1% tryptone , 0.25% agar) in 6-well plates. Each well contained either 0.3% DMSO or 71 µM piericidin A1, rotenone, or pyridaben. The plates were stored at 26°C for 24 hours before the diameter of swimming motility from the center was measured. To increase bacterial visibility, 24 mM MTT was added on top of the motility agar just before imaging.

Real-time PCR. Overnight bacterial cultures grown in M9 were backdiluted and grown in M9 at 37˚C to induce type III secretion, as described in (31), in the presence of DMSO, piericidin A1, rotenone, or pyridaben. RNA was isolated using an RNeasy Plus Micro Kit (Qiagen) according to the manufacturer's instructions. SYBR Green PCR master mix (Applied Biosystems) was used for qPCR reactions according to the manufacturer's instructions and a 60°C annealing temperature. Primers used are listed in Table S1. The YopE primers were designed using Primer 3 software (http://fokker.wi.mit.edu/primer3/input.htm). Results were analyzed using the Bio-Rad CFX software.

Immunofluorescence staining of YscF. Visualization of YscF was carried out as

previously described (32) with the following modifications: coverslips were blocked overnight with PBST + 3% BSA (PBST/BSA) at 4°C. Blocking solution was removed and anti-YscF primary antibody was added at 1:10,000 in PBST/BSA and rocked at 4°C for 4 hours. Coverslips were carefully rinsed in ice cold PBST + 0.1% tween-20 several times, and were incubated with Alexa fluor 594 anti-rabbit secondary antibody (Invitrogen) at 1:10,000 in PBST/BSA and rocked at 4°C for 3 hours followed by rinsing again in ice cold PBST + 0.1% tween- 20 several times. Coverslips were then stained for nuclear material with Hoechst 33342 (Thermo Scientific) at 1:10,000 in PBST/BSA and left in the dark at RT for 30 minutes. Coverslips were washed in ice cold PBST + 0.1% tween-20 several times, allowed to dry briefly, were mounted onto glass coverslips with Prolong Gold (Thermo Scientific), and sealed with clear nail polish. Images were taken with the Zeiss Axioimager Z2 widefield microscope under 63x/1.4 oil immersion using Zen software, and were pseudocolored and merged in FIJI. The conditions were blinded, and the numbers of puncta associated with a single bacterium were counted.

YscK, YscL, YscD, and YscQ analysis. *Y. enterocolitica* expressing N-terminal fluorescent fusions of cytosolic T3SS components, EGFP-YscK, mCherry-YscL, EGFP-YscQ, or EGFP-YscD joined by a glycine-rich flexible 13 amino acid linker and expressed from the native genetic environment on the virulence plasmid (33, 34) were grown over night in brain heart infusion (BHI) broth containing nalidixic acid (35 μg/ml) and diaminopimelic acid (80 μg/ml). Main cultures were inoculated to an optical density of 0.12 in the same medium, additionally complemented with 5mM

EDTA, 10mM MgCl2, and 0.4% glycerol. Cultures were grown for 1.5 hrs at 28°C. 71 μM piericidin A1 or the equivalent volume of DMSO were added and the cultures were switched to 37°C for another 3 hrs. 1.5 μl of the culture were layered on a patch of 1.5% agarose in M22 medium supplemented with 80 μg/ml diaminopimelic acid, 5mM EDTA, 10mM MgCl2, 0.4% glycerol, and either 71 μM piericidin A1 or the equivalent volume of DMSO. Fluorescence and DIC images of z stacks (n=4, □z=250 nm) were taken on a Deltavision optical sectioning microscope (Applied Precision) equipped with a UPlanSApo 100 × 1.35 oil objective (Olympus). DIC frames were imaged for 10 ms, and mCherry and GFP frames were imaged for 1 s, using appropriate filter sets. Detection and quantification of fluorescent foci was performed as in (35).

Statistical analysis. Statistical analysis was performed using KaleidaGraph (Synergy Software) or GraphPad as specified in each figure legend.

RESULTS

Complex I inhibition by piericidin does not underlie its ability to block type III secretion

Piericidin A1 inhibits complex I of the electron transport chain in at least some bacterial species (3). Type III secretion requires a proton motive force to translocate substrates; treatment with the proton uncoupler CCCP abolishes secretion (Fig. S1A). Therefore, it is possible that piericidins block type III secretion by blocking proton motive force generation. To investigate this possibility, we tested the effect of

pyridaben and rotenone, two structurally distinct compounds with complex I inhibitory activity in mitochondria and certain bacteria, on Yop secretion in *Y. pseudotuberculosis*. Pyridaben and rotenone did not significantly block secretion of the T3SS effector YopE, while piericidin inhibited 50% of YopE secretion (Fig. S1B), suggesting that compounds with complex I inhibitory activity do not all inhibit type III secretion.

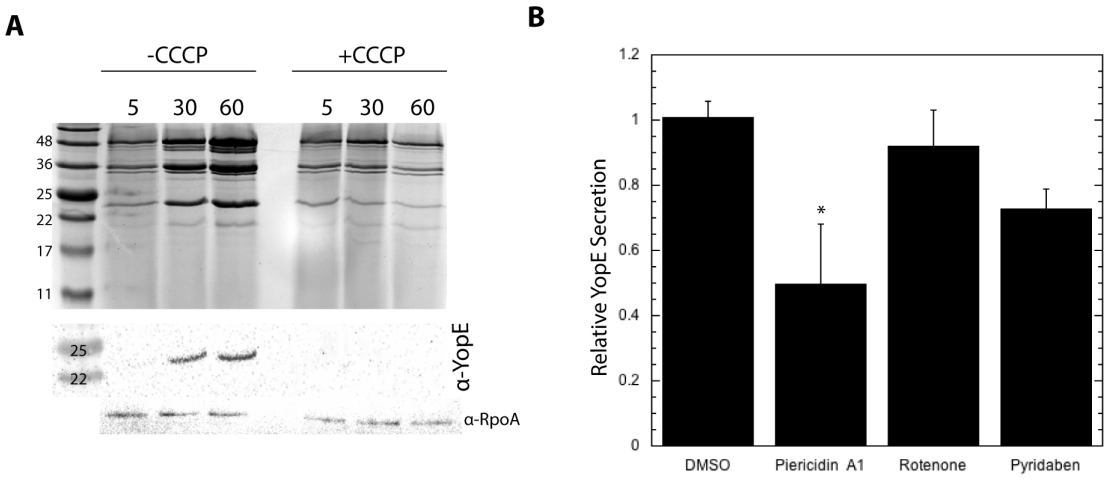

FIG S1 (A) *Y. pseudotuberculosis* type III secretion was determined after the addition of CCCP, a proton decoupler, to test the role of proton motive force in type III secretion. (B) *Y. pseudotuberculosis* type III secretion of YopE was measured in the presence of piericidin A1 and the complex I inhibitors rotenone and pyridaben. Shown are the average results of five independent experiments ± the standard error of the mean. *, $P < 0.03$ by analysis of variance with Tukey's honestly significant difference *post hoc* test on all four samples.

As both non-flagellar and flagellar T3SSs require the proton motive force, we tested whether piericidin A1 affected *Y. pseudotuberculosis* motility in a soft agar migration assay. Piericidin A1 (71 μM) did not inhibit *Yersinia* motility, while the proton gradient uncoupler CCCP did (Fig. 1A). In addition, piericidin A1 did not alter the

speed or directionality of *Yersinia* motility, as observed by video microscopy (data not shown). Finally, we evaluated any effect piericidin A1 may have on membrane potential directly using the membrane potential indicator dye JC-1 and observed no significant change (Fig. 1B). These data indicate that piericidin A1 does not inhibit the flagellar T3SS and that piericidins do not prevent generation of a proton motive force needed to support type III secretion in *Yersinia*. Furthermore, these results suggest that piericidin A1 does not target a structure shared between the flagellar and non-flagellar Ysc T3SS nor a regulator shared between the two secretion systems, such as Hfq (36).

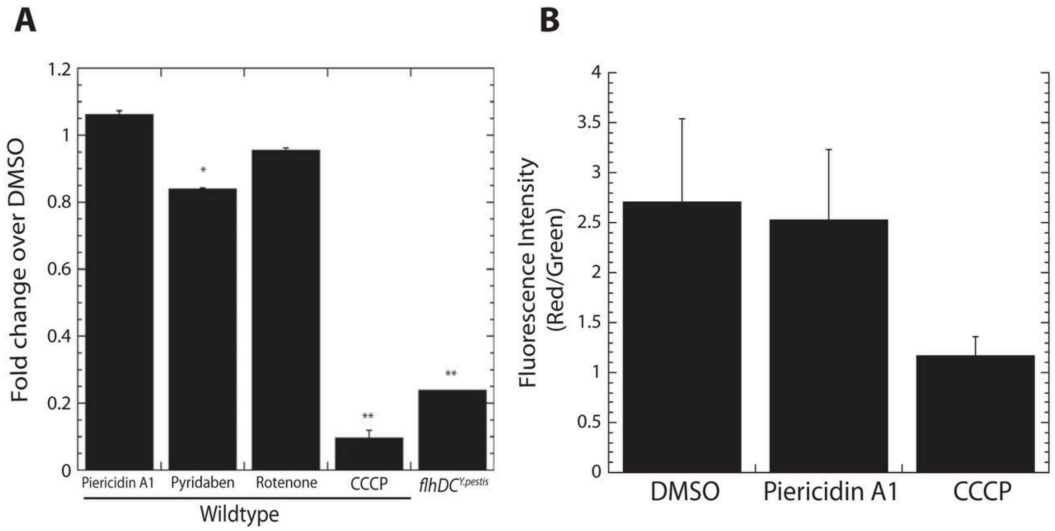

FIG 1 Complex I inhibition activity of piericidin A1 does not underlie its T3SS inhibitory activity. (A) Motility was analyzed by spotting 1-µl aliquots of WT *Y. pseudotuberculosis* or a nonmotile mutant onto motility medium in the presence of DMSO or piericidin A1 (71 µM). Shown are the average results of four independent experiments ± the standard error of the mean. *, $P < 0.001$ by analysis of variance with Bonferroni's *post hoc* test. (B) The proton motive force of *Y. pseudotuberculosis* was measured in the presence of DMSO or piericidin A1 (71 µM) with JC-1 dye. The protonophore CCCP was added as a negative control. The ratio of red/green fluorescence intensity indicates membrane potential. Shown are the average results of two independent experiments.

Coenzyme Q shares some structural similarity with piericidins and associates with complex I during electron transport (37) (Fig. S2). Coenzyme Q is also sold as a dietary supplement for human consumption (38). Therefore, we tested the ability of coenzyme Q to inhibit type III secretion in *Yersinia*. Unlike piericidin, coenzyme Q did not inhibit YopE secretion in *Y. pseudotuberculosis* (Fig. S3).

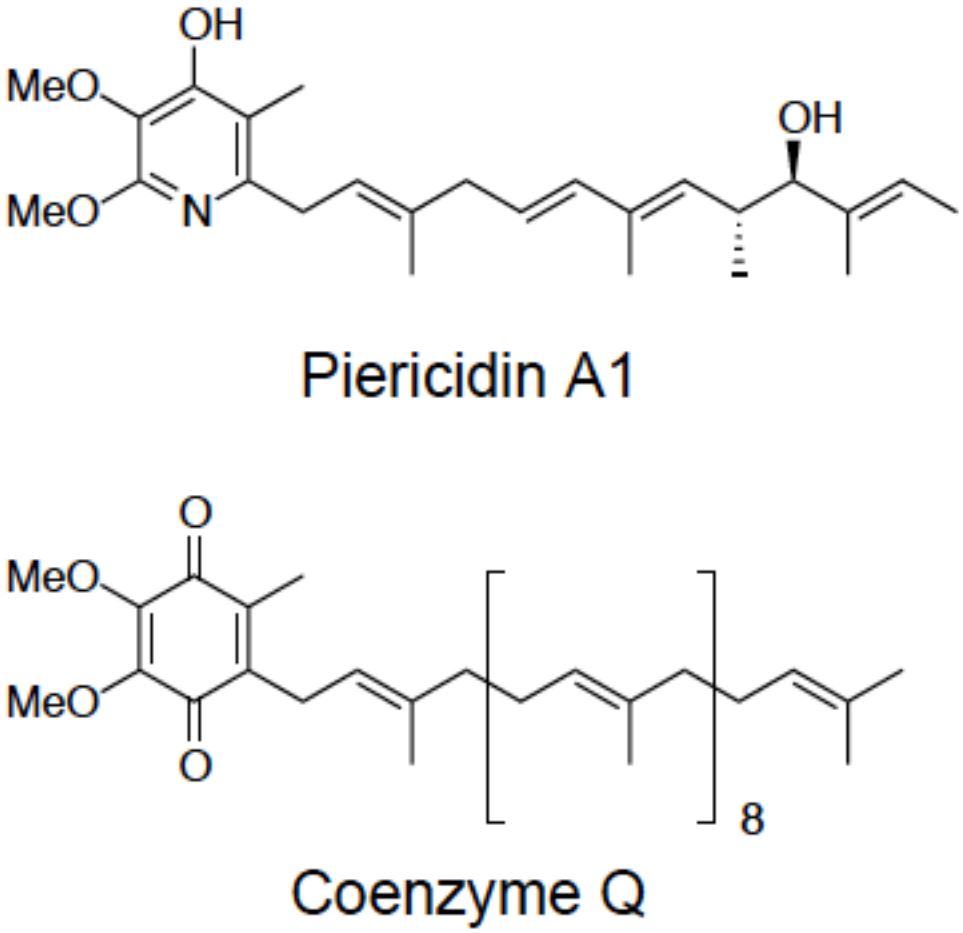

FIG S2 Structures of piericidin A1 and coenzyme Q

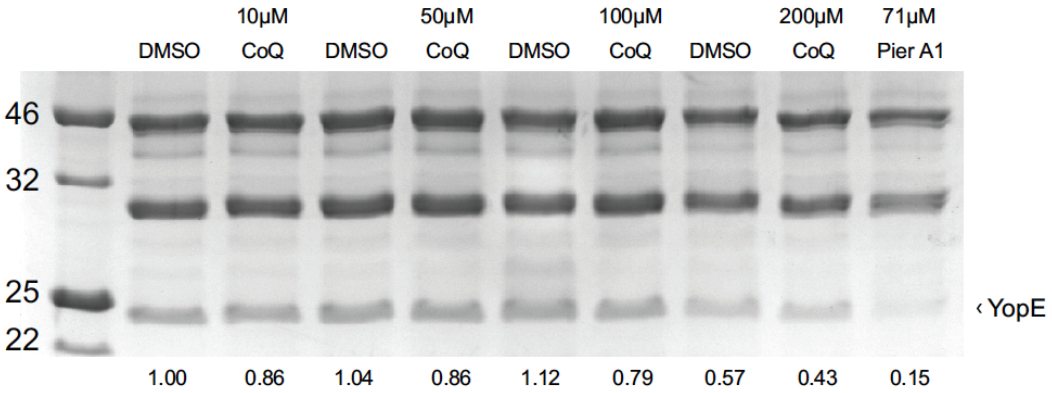

FIG S3 Coenzyme Q does not inhibit the Ysc T3SS. Yop secretion from *Y. pseudotuberculosis* grown under T3SS-inducing conditions in the presence of coenzyme Q, piericidin A1, or DMSO (control) was analyzed. Each concentration of coenzyme Q used is shown with the corresponding equal-volume DMSO control. At higher DMSO percentages, bacterial fitness is compromised, leading to decreased secretion, as seen with the largest DMSO volume used. The image shown is representative of three biological replicates.

Piericidin A1 inhibits the *Y. pseudotuberculosis* and *Y. enterocolitica* Ysc T3SS, but not the *Y. enterocolitica* Ysa T3SS

As we did not observe inhibition of the flagellar T3SS by piericidin A1, we tested its ability to inhibit the activity of T3SSs more closely related to the *Y. pseudotuberculosis* Ysc T3SS. Piericidin A1 reduced YopE secretion in *Y. enterocolitica* by 80% through the Ysc family T3SS in that organism (Fig. 2AB), similar to its previously reported effect on YopE secretion in *Y. pseudotuberculosis* (Fig. 2A) (9). However, piericidin A1 did not block ExoU or ExoT secretion in *Pseudomonas aeruginosa* (Fig. 2C), suggesting that piericidin does not inhibit the *Pseudomonas* T3SS, which is closely related to the Ysc T3SS (39). *P. aeruginosa* is known to exclude many antibiotics (40). Therefore, if the piericidin target of action is

intracellular, it is possible that lack of target accessibility explains why piericidin cannot inhibit the *P. aeruginosa* T3SS.

In order to test the ability of piericidin to block a T3SS outside the Ysc family in an organism where the target is known to be accessible, we took advantage of the fact that *Y. enterocolitica* encodes a second T3SS on its chromosome, called the Ysa system (41, 42). The Ysa T3SS is induced under high salt conditions at low temperatures (26˚C), reflecting its possible role during early stages of infection (41). We used a *Y. enterocolitica yscL* mutant defective in the Ysc T3SS to focus on the Ysa T3SS. We found that piericidin did not affect levels of secreted Ysa effector proteins called Ysps (Fig. 2D). As a control, the *yscL* mutant did not show Ysp secretion under low salt conditions. Lastly, a *ysaT* mutant, previously shown to be defective in Ysa secretion (29), did not secrete Ysps. These data show that while piericidin can inhibit the Ysc T3SS in *Y. enterocolitica*, this compound cannot block the Ysa T3SS in the same organism.

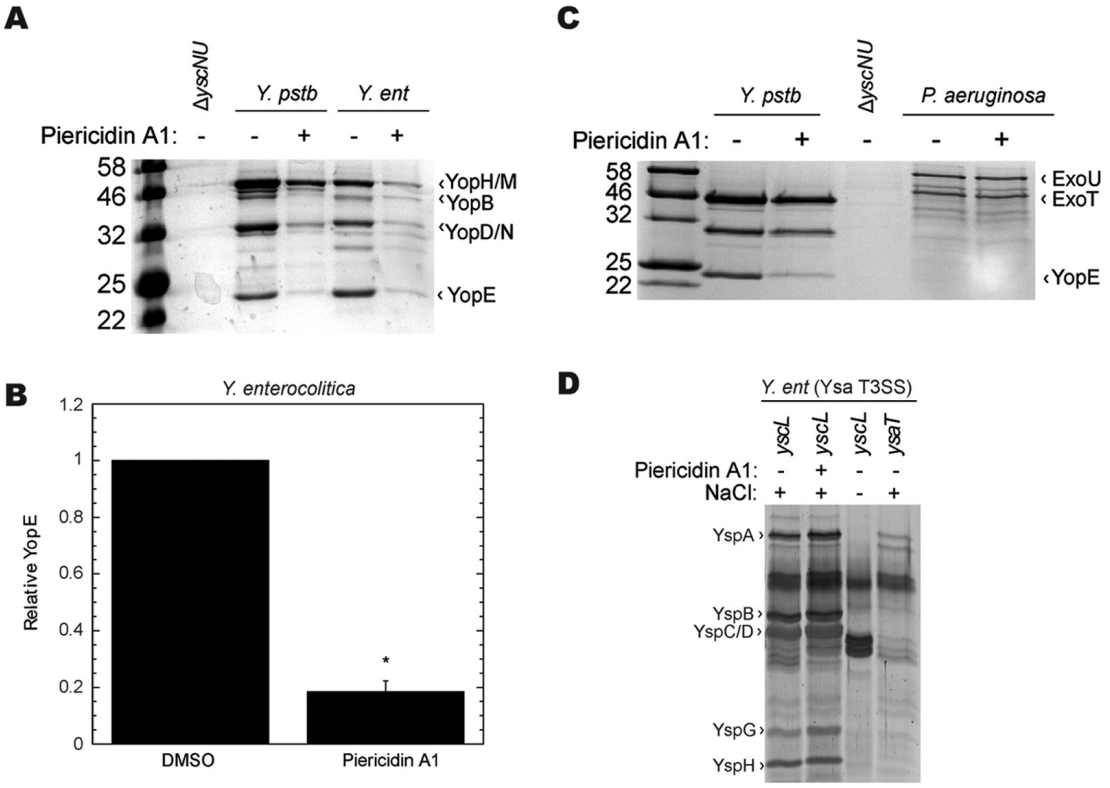

FIG 2. Piericidin A1 blocks the Ysc T3SS in enteropathogenic *Yersinia* but does not block the Ysc family T3SS in *Pseudomonas aeruginosa* nor the Ysa T3SS in *Y. enterocolitica*. Relative efficiency of effector protein secretion into the culture supernatant was analyzed following bacterial growth under T3SS-inducing conditions in the presence or absence of piericidin A1 (71µM). The secretome was precipitated with trichloroacetic acid and visualized by SDS-PAGE separation and staining with (A-C) coomassie blue or (D) SYPRO® Ruby. **A-C)** Ysc family T3SS: *Y. pseudotuberculosis*, *Y. enterocolitica*, and *P. aeruginosa* were grown in low calcium media at 37˚C. The *Y. pseudotuberculosis* Δ*yscNU* strain was used as a negative control for Yop secretion, as it does not express a Ysc T3SS (52). * $p<0.0001$ Student *t* test. **D)** Ysa T3SS: *Y. enterocolitica* was grown under high salt conditions at 26˚C.

Piericidin A1 traps T3SS effector proteins inside bacterial cells independently of the YopN, YopD, and YopK T3SS regulatory proteins

To begin to understand how piericidin inhibits *Yersinia* type III secretion, we tested whether piericidin A1 blocks type III secretion by blocking expression of T3SS structural components or effectors. Transcript levels of the T3SS ATPase YscN and

the effector YopE were unchanged following piericidin A1 treatment (Fig. S4), suggesting that piericidin A1 prevents T3SS activity through a post-transcriptional mechanism. Therefore, we tested whether piericidin A1 could prevent YopE protein expression by analyzing levels of secreted and intracellular YopE. While the pool of secreted YopE decreased upon piericidin treatment, intracellular YopE levels were significantly higher (Fig. 3A), indicating that piericidin A1 blocks secretion, not translation, of Yops. To determine if piericidin A1 blocks Yop secretion by targeting a T3SS regulatory component, we tested the ability of piericidin A1 to inhibit Yop secretion in *Y. pseudotuberculosis* mutants lacking YopD, YopK, or YopN. In all cases, piericidin A1 was able to inhibit Yop secretion (Fig. 3B), and YopE buildup in the bacterial cytosol remained unaffected (Fig. S5 and Fig. 3B). This indicates that piericidin inhibits the T3SS independently of the YopD, YopK, and YopN regulators.

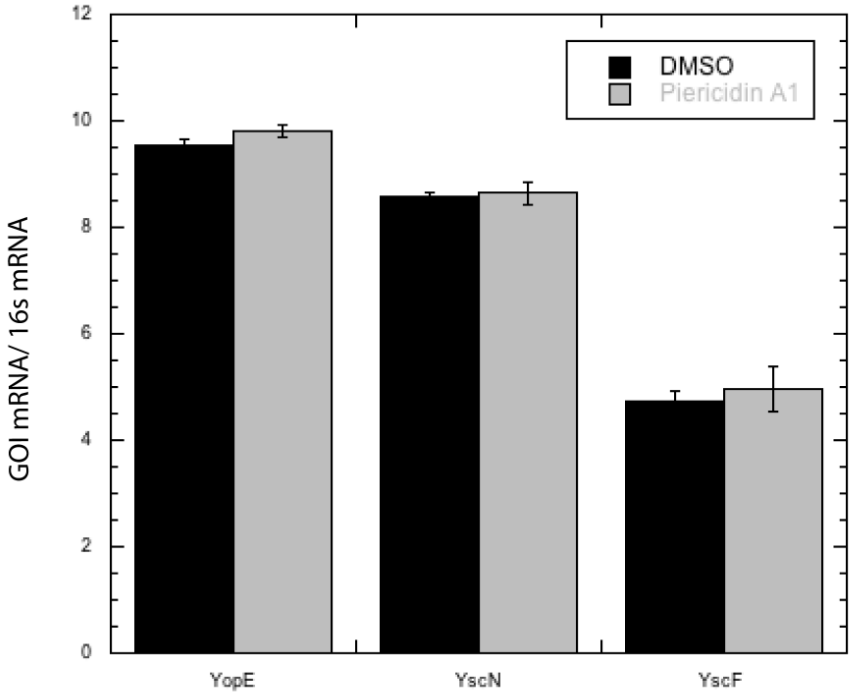

FIG S4 Piericidin A1 does not affect T3SS gene transcript levels. *Y. pseudotuberculosis* was grown in M9 medium at 37°C, and transcript levels were measured by real-time PCR as described in Materials and Methods. The average value ± the standard error of the mean of three independent experiments is shown. 16S rRNA levels were used as the reference.

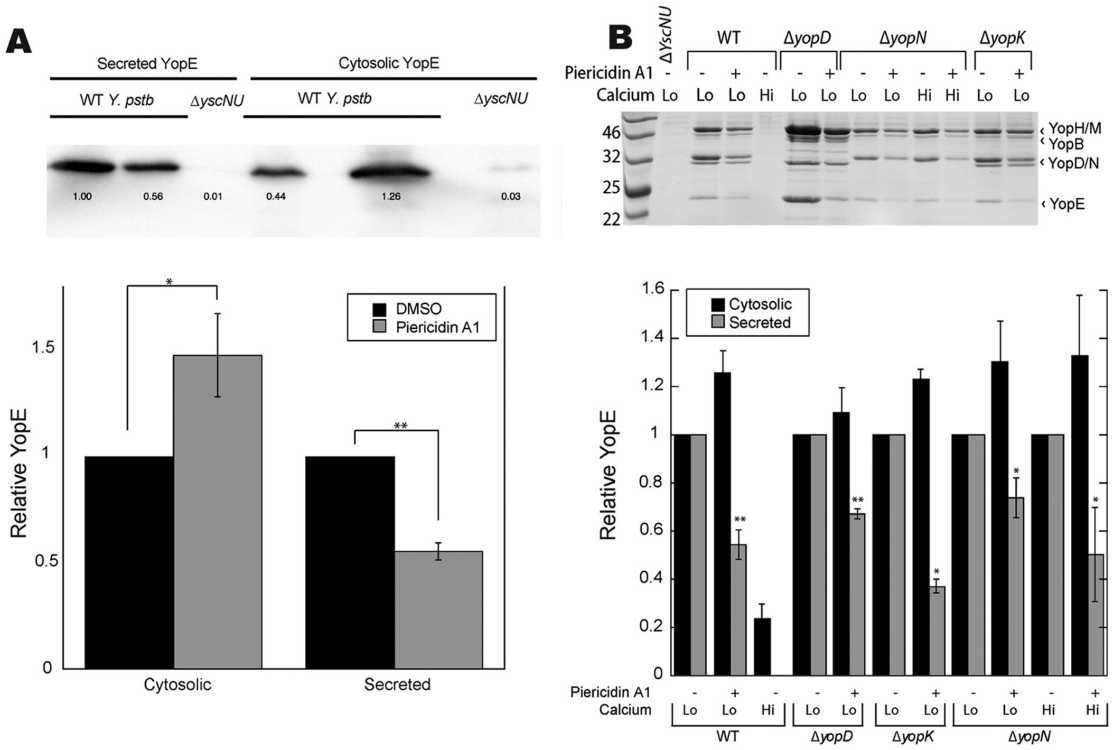

FIG 3. Piericidin A1 traps YopE in the bacterial cytoplasm. A) Cytosolic and secreted YopE was detected by immunoblot for wildtype *Y. pseudotuberculosis* treated with DMSO or piericidin A1 (71µM). Shown are the averages from 8-9 independent experiments ± sem. * $p<0.03$, ** $p<0.0001$ Student *t* test. **B)** Representative SDS-PAGE gel showing the secretome of WT and T3SS regulatory mutants of *Y. pseudotuberculosis* treated with piericidin A1 (71µM) under high and low calcium conditions (top panel). Quantitation of cytosolic and secreted YopE for the same strains and conditions (lower panel) from four independent experiments ± sem. * $p<0.05$, ** $p\leq0.0005$ Student *t* test.

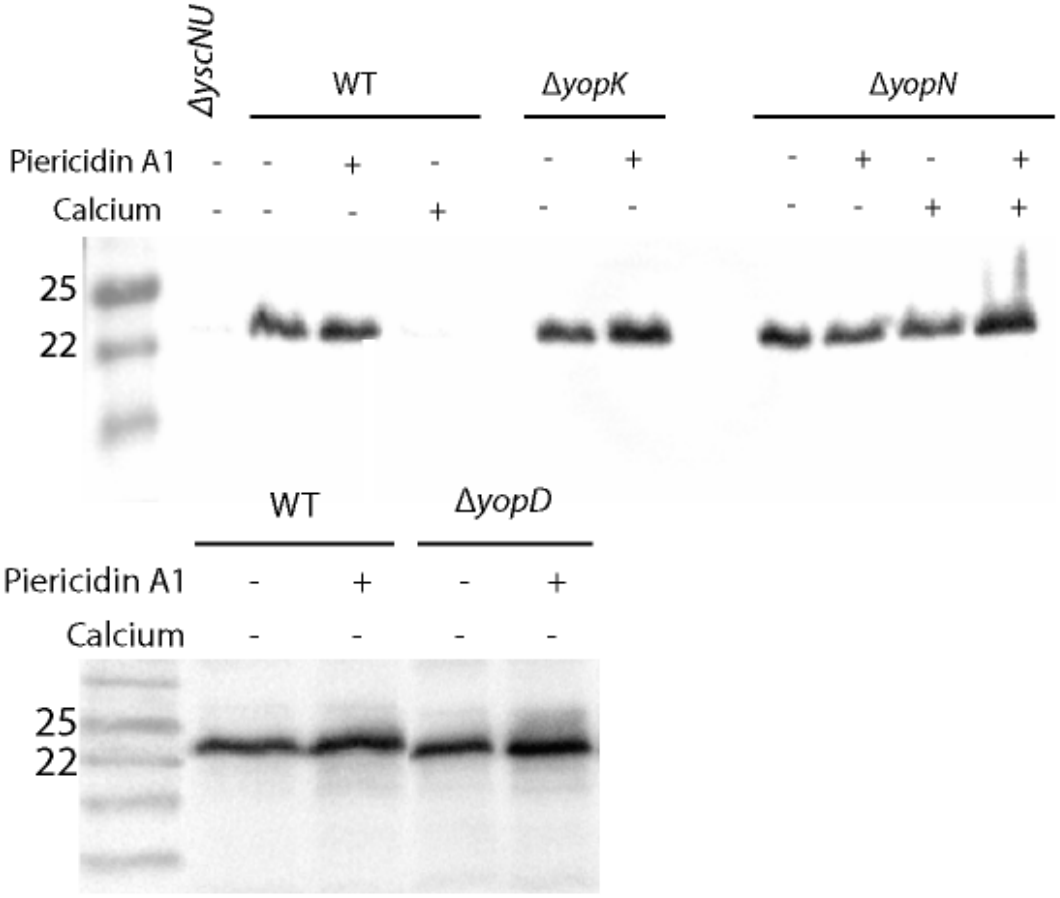

FIG S5 Piericidin A1 leads to accumulation of Yops in the bacterial cytosol of WT *Y. pseudotuberculosis*, as well as a *Yersinia* mutant lacking the regulatory protein YopD, YopK, or YopN. These are additional biological replicates of the experiments shown in **FIG 3B.**

Piericidin A1 decreases the number of T3SS needles associated with the bacterial surface but does not alter localization of basal body components

To determine if piericidin A1 inhibits Yop secretion by blocking assembly of the T3SS needle, we incubated *Y. pseudotuberculosis* in the presence or absence of piericidin A1 and measured the number of T3SS needle complexes by staining the bacteria using antibodies recognizing the needle subunit YscF. One antibody, raised

against full-length, purified YscF (43), was previously used to analyze YscF puncta in *Y. pseudotuberculosis* (32), while the other antibody was raised against a YscF peptide for this study (see Materials and Methods). Regardless of which antibody was used, piericidin A1 reduced the number of bacterially-associated YscF puncta by approximately half (Fig. 4 and data not shown), suggesting that piericidin inhibits Yop secretion by blocking formation of T3SS complexes, blocking secretion of needle subunits, and/or by leading to assembly of non-functional needles that are not recognized by anti-YscF antibodies. We compared this phenotype to that of an inhibitor whose molecular target has been suggested through suppressor mutation analysis to be the YscF homolog in *Pseudomonas aeruginosa,* PscF (44). Piericidin A1 reduced YscF puncta to the same magnitude as the PscF phenoxyacetamide inhibitor, MBX1641 (Fig. 4).

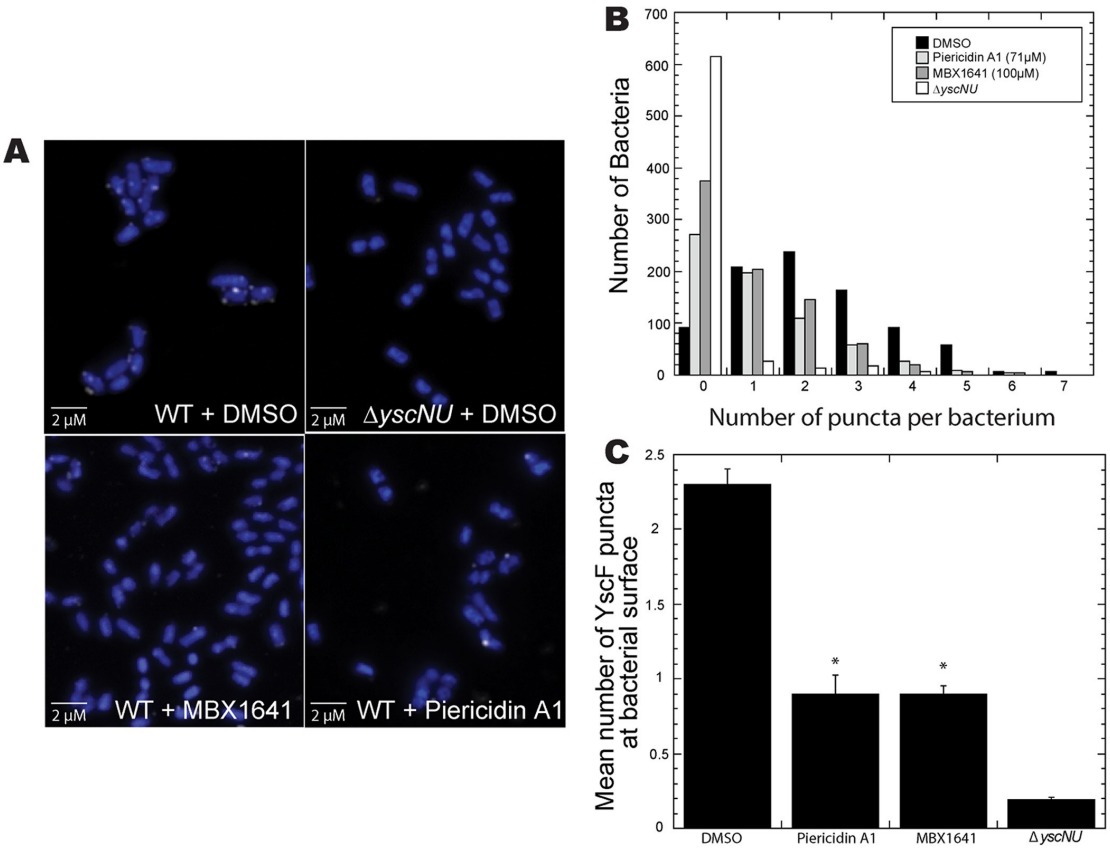

FIG 4. Treatment of *Yersinia* with piericidin A1 leads to a decrease in bacterially-associated YscF puncta. A) Representative confocal microscopy images of *Y. pseudotuberculosis* stained for T3SS puncta following treatment with DMSO or T3SS inhibitors MBX-1641 and piericidin A1 (71μM). **B)** Histogram showing the number of T3SS puncta per bacterium following treatment with DMSO or T3SS inhibitors. **C)** Average number of T3SS puncta per bacterium following drug treatment from four independent experiments ± sem. * $p<0.0001$ ANOVA with Bonferroni post-hoc test.

To determine whether the reduction in needle numbers was caused by (or accompanied by) a corresponding reduction in basal body assembly, we analyzed subcellular localization of three sorting platform proteins, YscK, YscL, and YscQ, and of the basal body ring YscD by monitoring EGFP-linked alleles of these proteins in *Y. enterocolitica* (35). While we observed a slight increase in spot intensity upon

piericidin A1 treatment compared to the DMSO control, there was no statistically significant change in the number of spots per cell length (Fig. S6), suggesting that the main effect of piericidin is not on the level of localization of the cytosolic or basal body T3SS components. Instead, piericidin A1 may block secretion of T3SS cargo including YscF or YscF needle assembly.

Piericidin A1 blocks YscF higher order structure formation and decreases secretion of middle and late T3SS substrates

In an attempt to determine if piericidin affects YscF needle polymerization, we employed a BS^3 crosslinking assay (30). We detected a decrease in higher order YscF polymers between the control and piericidin treated bacteria (Fig. 5A), suggesting that piericidin A1 decreases YscF needle assembly. In further support of this conclusion, we observed an accumulation of monomeric YscF in the supernatant upon piericidin A1 treatment (Fig. 5B). Taken together, these data support a model in which piericidin A1 prevents proper assembly of YscF polymers, resulting in an accumulation of monomeric YscF in the supernatant.

The T3SS basal body secretes its cargo in a hierarchical manner, with early (ex-YscF), middle (ex-LcrV), and late (ex-YopE) substrates (45). As piericidin A1 caused an increase in monomeric YscF, decreased polymeric YscF, and decreased YopE in the supernatant, we tested the effect of piericidin A1 on secretion of LcrV and YopD. As seen for late substrates, secretion of LcrV and YopD was decreased upon piericidin A1 treatment (Fig. 5B and data not shown), suggesting that piericidin

blocks YscF needle assembly, thereby inhibiting secretion of middle and late T3SS substrates.

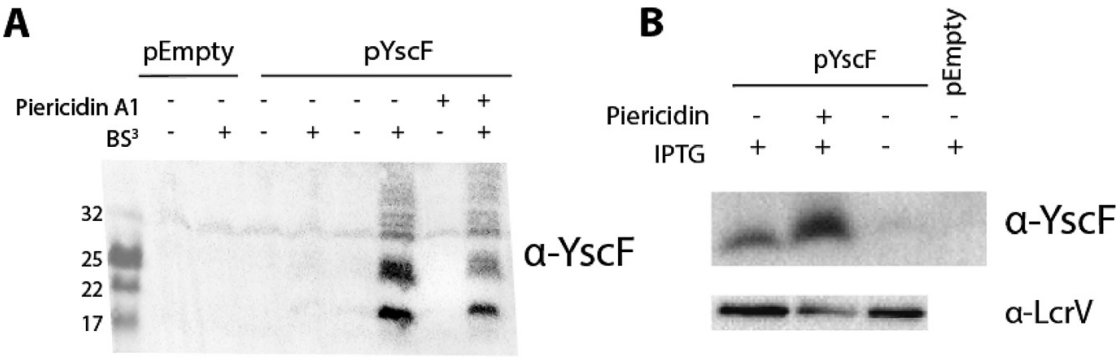

FIG 5. Treatment of *Yersinia* with piericidin A1 effects YscF needle polymerization. A) Crosslinking of YscF polymers on *Y. pseudotuberculosis* in the presence or absence of piericidin A1 (71μM). Image representative of five independent replicates. **B)** Secreted YscF and LcrV was detected by immunoblot after trichloroacetic acid precipitation of supernatants from *Y. pseudotuberculosis* treated with DMSO or piericidin A1 (71μM).

Piericidin A1 inhibition of type III secretion is reversible, and this reversibility is independent of new protein synthesis

We next sought to determine whether piericidin inhibition of Yop secretion was reversible. We incubated *Y. pseudotuberculosis* in the presence of piericidin A1 for two hours under T3SS inducing conditions, washed to remove the compound, and allowed the bacteria to secrete T3SS effectors in fresh low calcium media with or without piericidin A1 for an additional 45 minutes. As expected, *Y. pseudotuberculosis* incubated with piericidin A1 for the duration of the experiment significantly reduced secretion of YopE (Fig. 6A). It should be noted that cells that were only exposed to piericidin A1 during the last 45 minutes of the experiment still had a significant decrease in secretion, indicating that piericidin can inhibit type III secretion after T3SS expression has already been induced. However, if piericidin was

removed for the final 45-minute incubation, YopE secretion levels approached that of control bacteria treated with DMSO for the entire experiment (Fig. 6A). These data indicate that the action of piericidins on the T3SS is reversible, either because the piericidin A1 block in YscF needle assembly is reversible or because new needle complexes are assembled during the piericidin-free 45-minute incubation. To address the latter possibility**,** we repeated the washout treatment in the presence or absence of the translation inhibitor chloramphenicol during the final 45-minute incubation post removal of piericidin A1 and analyzed YscF puncta. While chloramphenicol significantly decreased the number of YscF puncta associated with bacteria not exposed to piericidin A1, chloramphenicol did not alter the number of YscF puncta on *Yersinia* pre-treated with piericidin A1 (Fig. 6B). These data suggest that reversal of piericidin A1 inhibition by washing away the compound does not depend on new protein synthesis; rather, it allows for previously constructed needle complexes to regain secretion activity once piericidin is removed or for new needles to be polymerized from preformed needle subunits. Indeed, we observed an accumulation of cytoplasmic YscF in piericidin-treated bacteria under T3SS-inducing conditions (Fig. 6D), indicating that while YscF can be secreted in the presence of piericidin A1, the block in polymerization may eventually lead to a back-up of YscF in the cytosol. This cytoplasmic pool may then be secreted and polymerized into a functional T3SS needle once piericidin is removed.

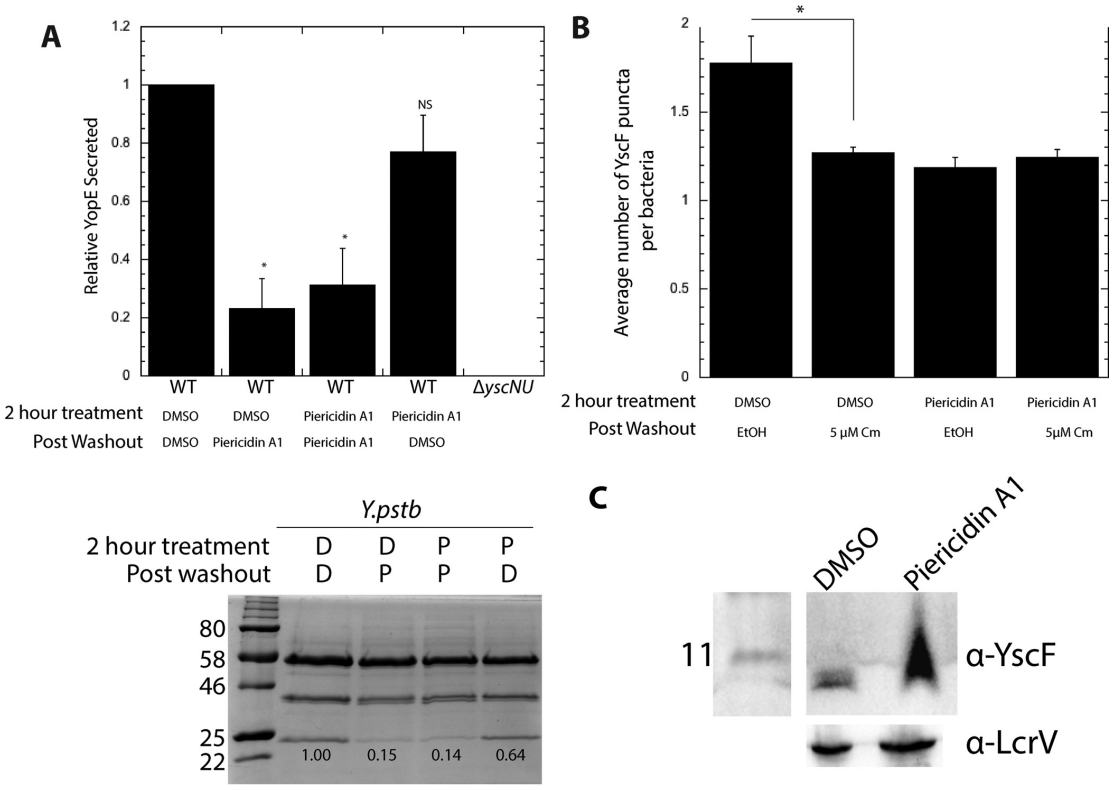

FIG 6. The action of piericidin A1 on YopE secretion is independent of new protein synthesis. A) Relative levels of secreted YopE from *Y. pseudotuberculosis* incubated with piericidin A1 (71μM) or DMSO for an initial two hour incubation, followed by a washout and resuspension in fresh low calcium media and either DMSO or piericidin A1 (71μM) for another 45 minutes. Shown are the averages from four independent experiments ± sem (top panel) and a representation gel (lower panel). * $p<0.002$ ANOVA Tukey HSD post-hoc test on all four samples. **B)** Average number of YscF puncta following treatment with piericidin A1 (71μM) and/or the translation inhibitor chloramphenicol. Shown are the averages from four independent experiments ± sem. * $p<0.02$ Student *t* test. **C)** Cytosolic YscF was detected by immunoblot for *Y. pseudotuberculosis* pYscF treated with DMSO or piericidin A1 (71μM). YscF expression was induced with 10μM IPTG.

DISCUSSION

In this study we characterize the activity of piericidin A1 as an inhibitor of the bacterial T3SS in *Yersinia pseudotuberculosis* and *Y. enterocolitica*. Piericidin A1

was originally described as an inhibitor of complex I in the mitochondrial electron transport chain (2) and in some prokaryotes (3). However, the data presented here demonstrate that piericidin A1 inhibits the T3SS independently of complex I. In addition, piericidin A1 was shown to affect quorum sensing pathways in *Erwinia carotovora* (8). However, studies on quorum sensing in *Yersinia pestis* indicate that quorum sensing negatively regulates expression of T3SS genes (46). As our study shows that piericidin A1 does not affect T3SS gene expression, piericidin activity on the *Yersinia* T3SS is predicted to be independent of any effect on quorum sensing. Instead, piericidin blocks assembly of the *Yersinia* YscF needle and subsequently secretion of middle and late T3SS substrates without altering localization of T3SS basal body components or inhibiting secretion of early substrates. Furthermore, the effect of piericidin is specific, as it does not influence the *Yersinia* Ysa or flagellar T3SSs. Thus, we propose that piericidins have an alternative molecular target specific to the Ysc T3SS in pathogenic *Yersinia* involved in YscF needle assembly.

Our data suggest that the molecular target of piericidin is unique to the Ysc secretion system and shared between the two enteropathogenic *Yersinia* species, but is either absent from or not well enough conserved in *P. aeruginosa*, which expresses a Ysc family T3SS. Alternatively, if piericidin must cross the bacterial cell envelope to carry out its T3SS inhibitory activity, *P. aeruginosa* may exclude or efflux piericidins. *P. aeruginosa* is known to have a high degree of drug resistance due to its unusually restrictive outer membrane permeability (40). However, we can conclude that piericidins do not inhibit the more distantly related *Y. enterocolitica* Ysa T3SS,

though piericidin can inhibit the Ysc T3SS in this species.

Piericidin treatment reduced the number of YscF needle puncta visible by fluorescence microscopy at the *Yersinia* surface. Each puncta may represent multiple T3SS needles located in proximity to one another (47), so our quantitation of approximately two puncta per bacterium likely underestimates the actual number of T3SS needles. Nevertheless, both piericidin and the needle subunit-targeting T3SS inhibitor MBX-1641 reduced the number of YscF puncta to less than one per bacterium. This suggests that both compounds either disrupt needle assembly or alter needle conformation such that needles cannot be readily recognized by our antibody. As we observed a similar piericidin-induced decrease in YscF puncta when a different antibody raised against full length YscF was used (43) (data not shown), the latter explanation is unlikely. Our data showing that piericidin decreases the abundance of higher order YscF polymers visible upon chemical crosslinking provides evidence for the former possibility.

Interestingly, while piericidin A1 treatment attenuates secretion of middle and late T3SS substrates, it does not decrease effector protein expression but instead causes an accumulation of effectors in the bacterial cytosol. These results are surprising given the known T3SS feedback loop; Yop mRNA levels are positively regulated by active secretion (48). YopD and LcrQ have been shown to prevent Yop translation prior to host cell contact and their subsequent secretion out of the bacterial cytosol through the T3SS relieves this repression (49). YopN is a regulatory protein involved in triggering effector secretion following host cell contact. Thus we

hypothesized that piericidin may block a regulatory pathway controlled by host cell contact, effectively causing a host contact "blind" phenotype. However, piericidin blocked type III secretion in the absence of YopD and YopN just as in wildtype bacteria. In addition, piericidin also inhibited type III secretion in the absence of YopK, a regulatory protein that controls T3SS translocon-mediated pore formation, a process recently linked to sensing host cell contact (50). Collectively, these data suggest that piericidin may block the ability of the YscF T3SS needle to mediate Yop secretion by altering YscF needle assembly in a reversible manner that does not impact the T3SS feedback loop.

Whether piericidins have potential as anti-microbial therapeutics remains unclear. While their specificity and efficacy on pre-formed T3SSs is attractive, they have two obvious limitations. First, the micromolar concentration required to observe T3SS inhibition are impractical for use in the clinic as a treatment or in prophylaxis. A second, and related, concern is the compound's toxicity to mammalian cells. Several groups have found piericidins to be poorly tolerated in animal models, likely due to their inhibition of murine mitochondrial complex I (51). A solution may lie in structure activity relationship (SAR) studies. Perhaps more promising is the use of these molecules as laboratory tools. Given the surprising result that piericidin blocks secretion of middle and late substrates without impacting the T3SS feedback loop, the compounds might be used to better understand T3SS regulatory pathways, as well as YscF needle formation and function. Furthermore the compounds could be used to explore host-pathogen interactions involving temporary T3SS inactivation, as type III

secretion can be restored by washing away the compound. Lastly, understanding why piericidin specifically targets the *Yersinia* Ysc T3SS may reveal novel mechanisms by which *Yersinia* have evolved to control the activity of this major virulence factor.

ACKNOWLEDGEMENTS

We thank Benjamin Abrams and the UCSC Life Sciences Microscopy Center for technical support with microscopy, Laura Kwuan for construction of the Δ*yopK* and Δ*yopD* mutants and the YopE qPCR primers, Glenn Young for the *Y. enterocolitica* strains and technical advice on the Ysp secretion assay, Joanne Engel for the *P. aeruginosa* strains, Joan Mecsas and Alison Davis for the ectopically expressed YscF strains and antibody against full length YscF, as well as the LcrV antibody, and members of the Auerbuch lab for helpful discussion. This work was supported by National Institutes of Health grant R01AI106930 (to V.A.), a Wellcome Trust Strategic Award (107457) supporting advanced microscopy at Micron Oxford (A.D), and by the National Human Genome Research Institute of the National Institutes of Health under Award Number R25HG006836 (to J.M.M.).

REFERENCES

1. **Lummen P.** 1998. Complex I inhibitors as insecticides and acaricides. Biochimica et biophysica acta **1364:**287-296.
2. **Hall C, Wu M, Crane FL, Takahashi H, Tamura S, Folkers K.** 1966. Piericidin A: a new inhibitor of mitochondrial electron transport. Biochemical and biophysical research communications **25:**373-377.
3. **Darrouzet E, Issartel JP, Lunardi J, Dupuis A.** 1998. The 49-kDa subunit of NADH-ubiquinone oxidoreductase (Complex I) is involved in the binding of piericidin and rotenone, two quinone-related inhibitors. FEBS letters **431:**34-38.
4. **Tocilescu MA, Zickermann V, Zwicker K, Brandt U.** 2010. Quinone binding and reduction by respiratory complex I. Biochimica et biophysica acta **1797:**1883-1890.
5. **Okun JG, Lummen P, Brandt U.** 1999. Three classes of inhibitors share a common binding domain in mitochondrial complex I (NADH:ubiquinone oxidoreductase). The Journal of biological chemistry **274:**2625-2630.
6. **Yagi T, Yano T, Di Bernardo S, Matsuno-Yagi A.** 1998. Procaryotic complex I (NDH-1), an overview. Biochimica et biophysica acta **1364:**125-133.
7. **Hwang JH, Kim JY, Cha MR, Ryoo IJ, Choo SJ, Cho SM, Tsukumo Y, Tomida A, Shin-Ya K, Hwang YI, Yoo ID, Park HR.** 2008. Etoposide-resistant HT-29 human colon carcinoma cells during glucose deprivation are

sensitive to piericidin A, a GRP78 down-regulator. Journal of cellular physiology **215:**243-250.

8. **Kang JE, Han JW, Jeon BJ, Kim BS.** 2016. Efficacies of quorum sensing inhibitors, piericidin A and glucopiericidin A, produced by *Streptomyces xanthocidicus* KPP01532 for the control of potato soft rot caused by *Erwinia carotovora subsp. atroseptica*. Microbiological research **184:**32-41.

9. **Duncan MC, Wong WR, Dupzyk AJ, Bray WM, Linington RG, Auerbuch V.** 2014. An NF-kappaB-Based High-Throughput Screen Identifies Piericidins as Inhibitors of the *Yersinia pseudotuberculosis* Type III Secretion System. Antimicrobial agents and chemotherapy **58:**1118-1126.

10. **Portaliou AG, Tsolis KC, Loos MS, Zorzini V, Economou A.** 2016. Type III Secretion: Building and Operating a Remarkable Nanomachine. Trends in biochemical sciences **41:**175-189.

11. **Wilharm G, Lehmann V, Krauss K, Lehnert B, Richter S, Ruckdeschel K, Heesemann J, Trulzsch K.** 2004. *Yersinia enterocolitica* type III secretion depends on the proton motive force but not on the flagellar motor components MotA and MotB. Infection and immunity **72:**4004-4009.

12. **Cornelis GR.** 2010. The type III secretion injectisome, a complex nanomachine for intracellular 'toxin' delivery. Biol Chem **391:**745-751.

13. **Cornelis GR.** 2006. The type III secretion injectisome. Nature reviews Microbiology **4:**811-825.

14. **Mattei PJ, Faudry E, Job V, Izore T, Attree I, Dessen A.** 2011. Membrane targeting and pore formation by the type III secretion system translocon. The FEBS journal **278:**414-426.

15. **Dewoody R, Merritt PM, Marketon MM.** 2013. YopK controls both rate and fidelity of Yop translocation. Molecular microbiology **87:**301-317.

16. **Anderson DM, Ramamurthi KS, Tam C, Schneewind O.** 2002. YopD and LcrH regulate expression of *Yersinia enterocolitica* YopQ by a posttranscriptional mechanism and bind to yopQ RNA. Journal of bacteriology **184:**1287-1295.

17. **Kopaskie KS, Ligtenberg KG, Schneewind O.** 2013. Translational regulation of *Yersinia enterocolitica* mRNA encoding a type III secretion substrate. The Journal of biological chemistry **288:**35478-35488.

18. **Armentrout EI, Rietsch A.** 2016. The Type III Secretion Translocation Pore Senses Host Cell Contact. PLoS Pathog **12:**e1005530.

19. **Kupferberg LL, Higuchi K.** 1958. Role of calcium ions in the stimulation of growth of virulent strains of *Pasteurella pestis*. Journal of bacteriology **76:**120-121.

20. **Higuchi K, Kupferberg LL, Smith JL.** 1959. Studies on the nutrition and physiology of *Pasteurella pestis*. III. Effects of calcium ions on the growth of virulent and avirulent strains of *Pasteurella pestis*. Journal of bacteriology **77:**317-321.

21. **Lee VT, Mazmanian SK, Schneewind O.** 2001. A program of *Yersinia enterocolitica* type III secretion reactions is activated by specific signals. Journal of bacteriology **183:**4970-4978.

22. **Plano GV, Schesser K.** 2013. The *Yersinia* pestis type III secretion system: expression, assembly and role in the evasion of host defenses. Immunologic research **57:**237-245.

23. **Auerbuch V, Golenbock DT, Isberg RR.** 2009. Innate immune recognition of *Yersinia pseudotuberculosis* type III secretion. PLoS Pathog **5:**e1000686.

24. **Kwuan L, Adams W, Auerbuch V.** 2013. Impact of host membrane pore formation by the *Yersinia pseudotuberculosis* type III secretion system on the macrophage innate immune response. Infect Immun **81:**905-914.

25. **Francis MS, Wolf-Watz H.** 1998. YopD of *Yersinia pseudotuberculosis* is translocated into the cytosol of HeLa epithelial cells: evidence of a structural domain necessary for translocation. Molecular microbiology **29:**799-813.

26. **Miller HK, Kwuan L, Schwiesow L, Bernick DL, Mettert E, Ramirez HA, Ragle JM, Chan PP, Kiley PJ, Lowe TM, Auerbuch V.** 2014. IscR is essential for *Yersinia pseudotuberculosis* type III secretion and virulence. PLoS Pathog **10:**e1004194.

27. **Zetterstrom CE, Hasselgren J, Salin O, Davis RA, Quinn RJ, Sundin C, Elofsson M.** 2013. The resveratrol tetramer (-)-hopeaphenol inhibits type III secretion in the gram-negative pathogens *Yersinia pseudotuberculosis* and *Pseudomonas aeruginosa*. PLoS One **8:**e81969.

28. **Aiello D, Williams JD, Majgier-Baranowska H, Patel I, Peet NP, Huang J, Lory S, Bowlin TL, Moir DT.** 2010. Discovery and characterization of inhibitors of *Pseudomonas aeruginosa* type III secretion. Antimicrob Agents Chemother **54:**1988-1999.

29. **Young BM, Young GM.** 2002. Evidence for targeting of Yop effectors by the chromosomally encoded Ysa type III secretion system of *Yersinia enterocolitica.* Journal of bacteriology **184:**5563-5571.

30. **Davis AJ, Mecsas J.** 2007. Mutations in the *Yersinia pseudotuberculosis* type III secretion system needle protein, YscF, that specifically abrogate effector translocation into host cells. J Bacteriol **189:**83-97.

31. **Miller HK, Kwuan L, Schwiesow L, Bernick DL, Mettert E, Ramirez HA, Ragle JM, Chan PP, Kiley PJ, Lowe TM, Auerbuch V.** 2014. IscR is essential for *Yersinia pseudotuberculosis* type III secretion and virulence. PLoS pathogens **10:**e1004194.

32. **Davis AJ, Diaz DA, Mecsas J.** 2010. A dominant-negative needle mutant blocks type III secretion of early but not late substrates in *Yersinia*. Mol Microbiol **76:**236-259.

33. **Diepold A, Amstutz M, Abel S, Sorg I, Jenal U, Cornelis GR.** 2010. Deciphering the assembly of the *Yersinia* type III secretion injectisome. The EMBO journal **29:**1928-1940.

34. **Diepold A, Armitage JP.** 2015. Type III secretion systems: the bacterial flagellum and the injectisome. Philosophical transactions of the Royal Society of London Series B, Biological sciences **370**.

35. **Diepold A, Kudryashev M, Delalez NJ, Berry RM, Armitage JP.** 2015. Composition, formation, and regulation of the cytosolic c-ring, a dynamic component of the type III secretion injectisome. PLoS biology **13:**e1002039.

36. **Schiano CA, Bellows LE, Lathem WW.** 2010. The small RNA chaperone Hfq is required for the virulence of *Yersinia pseudotuberculosis*. Infect Immun **78:**2034-2044.

37. **Friedrich T.** 2014. On the mechanism of respiratory complex I. Journal of bioenergetics and biomembranes **46:**255-268.

38. **Varela-Lopez A, Giampieri F, Battino M, Quiles JL.** 2016. Coenzyme Q and Its Role in the Dietary Therapy against Aging. Molecules **21**.

39. **Troisfontaines P, Cornelis GR.** 2005. Type III secretion: more systems than you think. Physiology (Bethesda) **20:**326-339.

40. **Hancock RE, Speert DP.** 2000. Antibiotic resistance in *Pseudomonas aeruginosa*: mechanisms and impact on treatment. Drug resistance updates : reviews and commentaries in antimicrobial and anticancer chemotherapy **3:**247-255.

41. **Haller JC, Carlson S, Pederson KJ, Pierson DE.** 2000. A chromosomally encoded type III secretion pathway in *Yersinia enterocolitica* is important in virulence. Molecular microbiology **36:**1436-1446.

42. **Matsumoto H, Young GM.** 2009. Translocated effectors of *Yersinia*. Curr Opin Microbiol **12:**94-100.

43. **Davis AJ, Mecsas J.** 2007. Mutations in the *Yersinia pseudotuberculosis* type III secretion system needle protein, YscF, that specifically abrogate effector translocation into host cells. Journal of bacteriology **189:**83-97.

44. **Bowlin NO, Williams JD, Knoten CA, Torhan MC, Tashjian TF, Li B, Aiello D, Mecsas J, Hauser AR, Peet NP, Bowlin TL, Moir DT.** 2014. Mutations in the *Pseudomonas aeruginosa* needle protein gene pscF confer resistance to phenoxyacetamide inhibitors of the type III secretion system. Antimicrobial agents and chemotherapy **58:**2211-2220.

45. **Dewoody RS, Merritt PM, Marketon MM.** 2013. Regulation of the *Yersinia* type III secretion system: traffic control. Front Cell Infect Microbiol **3:**4.

46. **Gelhaus HC, Rozak DA, Nierman WC, Chen D, Varga JJ, Zadeh M, Ulrich RL, Adamovicz JJ.** 2009. Exogenous *Yersinia pestis* quorum sensing molecules N-octanoyl-homoserine lactone and N-(3-oxooctanoyl)-homoserine lactone regulate the LcrV virulence factor. Microbial pathogenesis **46:**283-287.

47. **Kudryashev M, Diepold A, Amstutz M, Armitage JP, Stahlberg H, Cornelis GR.** 2015. *Yersinia enterocolitica* type III secretion injectisomes form regularly spaced clusters, which incorporate new machines upon activation. Molecular microbiology **95:**875-884.

48. **Deane JE, Abrusci P, Johnson S, Lea SM.** 2010. Timing is everything: the regulation of type III secretion. Cellular and molecular life sciences : CMLS **67:**1065-1075.

49. **Williams AW, Straley SC.** 1998. YopD of *Yersinia pestis* plays a role in negative regulation of the low-calcium response in addition to its role in translocation of Yops. Journal of bacteriology **180:**350-358.

50. **Armentrout EI, Rietsch A.** 2016. The Type III Secretion Translocation Pore Senses Host Cell Contact. PLoS pathogens **12:**e1005530.

51. **Mitsui T, Fukami J, Fukunaga K, Takahashi N, Tamura S.** 1970. Studies on Piericidin. Agricultural and Biological Chemistry **34:**1101-1109.

52. **Balada-Llasat JM, Mecsas J.** 2006. *Yersinia* has a tropism for B and T cell zones of lymph nodes that is independent of the type III secretion system. PLoS pathogens **2:**e86.

53. **Bliska JB, Guan KL, Dixon JE, Falkow S.** 1991. Tyrosine phosphate hydrolysis of host proteins by an essential *Yersinia* virulence determinant. Proceedings of the National Academy of Sciences of the United States of America **88:**1187-1191.

54. **Apodaca G, Bomsel M, Lindstedt R, Engel J, Frank D, Mostov KE, Wiener-Kronish J.** 1995. Characterization of *Pseudomonas aeruginosa*-induced MDCK cell injury: glycosylation-defective host cells are resistant to bacterial killing. Infection and immunity **63:**1541-1551.

55. **Liu PV.** 1966. The roles of various fractions of *Pseudomonas aeruginosa* in its pathogenesis. 3. Identity of the lethal toxins produced in vitro and in vivo. The Journal of infectious diseases **116:**481-489.

56. **Darwin AJ, Miller VL.** 1999. Identification of *Yersinia enterocolitica* genes affecting survival in an animal host using signature-tagged transposon mutagenesis. Molecular microbiology **32:**51-62.

57. **Young BM, Young GM.** 2002. YplA is exported by the Ysc, Ysa, and flagellar type III secretion systems of *Yersinia enterocolitica*. Journal of bacteriology **184:**1324-1334.